Geological Magazine

www.cambridge.org/geo

The physical volcanology of large-scale effusive and explosive silicic eruptions in southeastern Saurashtra, Deccan Traps

Anmol Naik[1], Hetu Sheth[1], Alok Kumar[2] and Janisar M. Sheikh[3]

[1]Department of Earth Sciences, Indian Institute of Technology Bombay, Powai, Mumbai, India; [2]Centre of Advanced Study in Geology, Institute of Science, Banaras Hindu University (BHU), Varanasi, India and [3]Department of Earth Sciences, Pondicherry University, Kalapet, Puducherry, India

Original Article

Cite this article: Naik A, Sheth H, Kumar A, and Sheikh JM (2023) The physical volcanology of large-scale effusive and explosive silicic eruptions in southeastern Saurashtra, Deccan Traps. *Geological Magazine* **160**: 1395–1416. https://doi.org/10.1017/S0016756823000432

Received: 24 December 2022
Revised: 13 May 2023
Accepted: 22 June 2023
First published online: 31 July 2023

Keywords:
rhyolite; lava; pyroclastics; continental flood basalt; volcanic rifted margin; Deccan Traps

Corresponding author: Hetu Sheth;
Email: hcsheth@iitb.ac.in

Abstract

Silicic magmatism, minor overall in the ~65.5 Ma Deccan Traps continental flood basalt (CFB) province of India, was widespread in the Saurashtra region. We describe the physical volcanology of silicic volcanics and dykes exposed around Rajula–Savarkundla–Gariyadhar–Talaja towns in southeastern Saurashtra. The silicic volcanics conformably overlie basaltic lavas, suggesting rapid subaerial volcanism, and the sequence shows gentle tectonic dips (~15°) towards the Arabian Sea. Rhyolites and dacites with preserved thicknesses of tens of metres show intense internal rheomorphic deformation, and a dacite shows a well-formed basal autobreccia. The rheomorphic rhyolites, and vitrophyres which often underlie them, lack vitroclasts (glass shards and pumice clasts). They have very similar mineral assemblages (quartz and alkali feldspar phenocrysts, and crystal cargoes dominated by calcic plagioclase and clinopyroxene or orthopyroxene, sometimes with olivine). The rheomorphic units are thus flood rhyolite and dacite lavas, apparently common in the northern-northwestern Deccan, and the vitrophyres their basal chilled parts. Tuffs (including crystal-vitric Plinian fallout ash) and eutaxitic ignimbrites formed from pyroclastic density currents; one tuff contains extraordinary numbers of lithophysae. Ridges of rhyolitic tuff breccias with pervasive secondary silicification and ferruginization represent pyroclastic eruptive fissures. The area thus records large-scale effusive and explosive silicic eruptions. Mafic and silicic dykes intrude the basaltic lavas and rarely the silicic volcanics. Mafic enclaves in several silicic dykes and some volcanics indicate magma mingling as a common phenomenon. The seaward-dipping volcanic units define a regional-scale flexure comparable to coastal flexures in CFB provinces worldwide, suggesting extensive block-faulting of this classical volcanic rifted margin.

1. Introduction

Widespread and voluminous silicic volcanic rocks overlie mafic lavas in many continental flood basalt (CFB) provinces of the world, such as the Karoo, Paraná–Etendeka, Deccan, British Palaeogene, Yemen, Ethiopian and Columbia River CFB provinces (e.g., Bryan *et al.* 2002, 2010). The petrogenesis of these silicic rocks involves diverse mechanisms such as fractional crystallization of basaltic melts, liquid immiscibility, partial melting of hydrothermally altered basalts and anatexis of continental crust and is, therefore, a topic of considerable interest (e.g. Rooney *et al.* 2010; Halder *et al.* 2021 and references therein). So is their physical volcanology: the silicic volcanics occur as lava flows and domes, formed by effusive eruptions (e.g., Polo *et al.* 2018), and as pyroclastic deposits, including ignimbrites, formed by explosive eruptions (e.g., Ayalew *et al.* 2002; Luchetti *et al.* 2018). Correctly identifying and interpreting these deposits and eruption types are important for understanding their likely environmental impact, given that explosive eruptions can inject ash and magmatic gases to much greater heights in the atmosphere than effusive eruptions, with correspondingly significantly wider distribution and environmental impact (e.g. Self, 2006; Cassidy *et al.* 2018). This is especially so when the CFB volcanism is known to have overlapped with a major mass extinction, such as the ~65.5 Ma Deccan Traps of India (Fig. 1) and the Cretaceous/Palaeogene (K/Pg) boundary mass extinction (e.g. Baksi, 2014).

In the Deccan Traps, covering 500,000 km^2 in west-central India (Fig. 1), silicic rocks are minor overall. However, rhyolites, dacites and granophyres are notable in the western and northern parts of the province and are particularly abundant in the Saurashtra peninsula in the northwest (Fig. 1) (e.g. Fedden, 1884; Subba Rao, 1971). Both silicic lavas and ignimbrites are recognized in these parts (Wakhaloo, 1967; Krishnamacharlu, 1974; Sheikh *et al.* 2020a, b; Naik *et al.* 2021), as is a giant (30 km-diameter) silicic caldera (Bandopadhyaya, 1976; Sheth *et al.* 2022a).

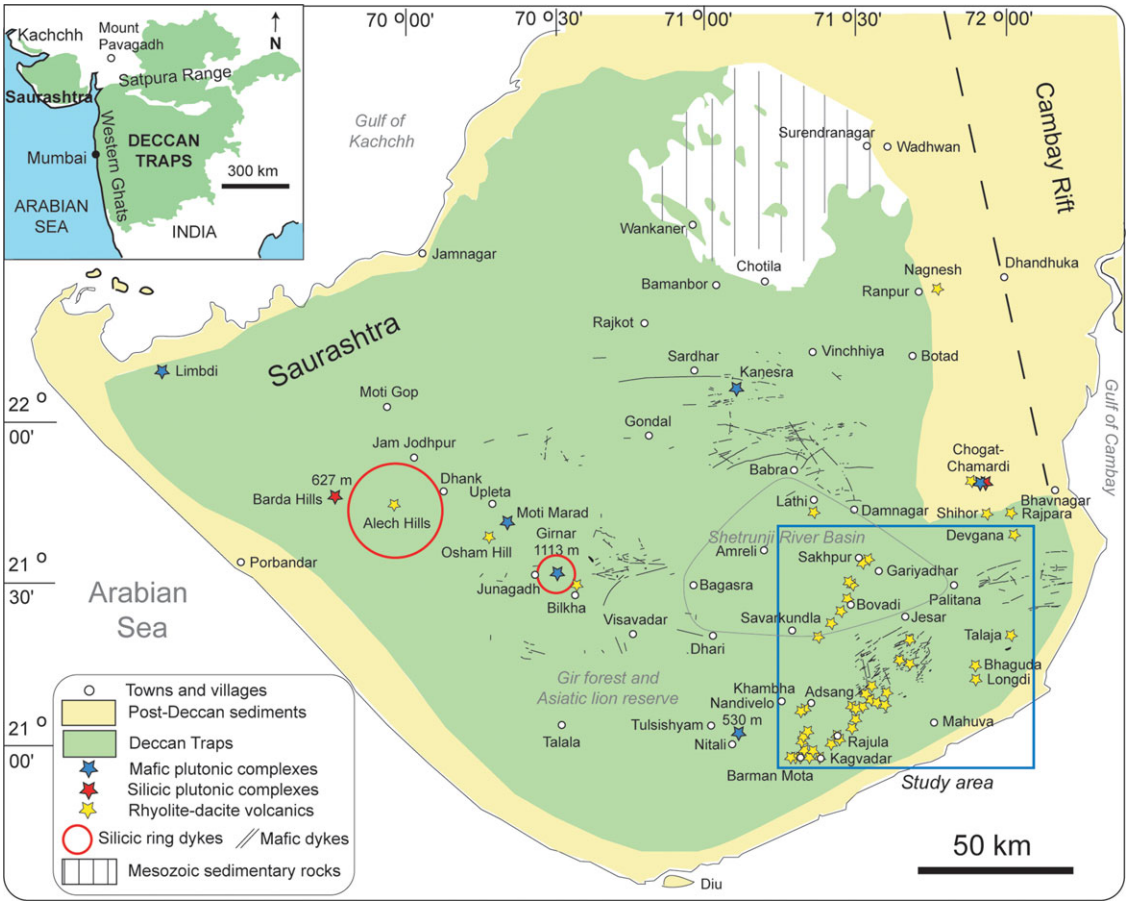

Figure 1. (Colour online) Geological maps of the Deccan Traps (inset, in green), and of Saurashtra, based on Cucciniello *et al.* (2022), showing important geological features and localities mentioned in the text. Red stars in the main map are plutonic complexes dominated by granophyre-microgranite (Barda, Chogat-Chamardi), and blue stars are plutonic complexes composed dominantly of gabbro with or without diorite (Girnar, Nandivelo, Kanesra, Moti Marad and Limbdi). Red circles mark large silicic ring dykes. Yellow stars are localities with significant silicic volcanics (based on Fedden, 1884 and our own field observations, see Naik *et al.* 2021 and references therein). Thin black lines are mafic dyke swarms studied in detail, including the Eastern Saurashtra, Central Saurashtra, Southeastern Saurashtra and circum-Girnar tholeiitic swarms (Cucciniello *et al.* 2020, 2022 and references therein). Box with blue border shows the area of the present study.

Silicic volcanic rocks are abundant around the towns of Rajula, Savarkundla, Gariyadhar and Talaja in southeastern Saurashtra (Fig. 1). They have been the subject of geological–geochemical accounts in varying degrees of detail (Krishnamacharlu, 1974; Misra, 1976, 1981, 1999; Chatterjee & Bhattacharji, 2001, 2004; Sethna *et al.* 2001; Kshirsagar *et al.* 2012; Sheikh *et al.* 2020a). In this work, we present new and detailed data on the locations, outcrop-scale structures and microscopic textures of previously described and undescribed silicic volcanic rocks (and associated dykes) of this area, along with new geological maps. These datasets help us to recognize large-scale effusive and explosive silicic eruptions and improve our understanding of Deccan silicic magmatism and CFB volcanism in general.

2. Geology and field observations

2.a. Geological background

Large parts of the Saurashtra (syn. Kathiawar) peninsula in the northwestern part of the Deccan Traps (Fig. 1) are topographically flat and low-lying (~100 m above sea level), and there are few thick vertical sections through the Deccan basalts. In the northern parts of Saurashtra, the basalts rest upon Mesozoic sedimentary rocks, whereas the coastal strips of Saurashtra expose Palaeogene and Quaternary carbonate sediments or alluvium (Fedden, 1884; Misra, 1981, 1999). Saurashtra has two special features compared to the Deccan Traps in general: (i) Tholeiitic rocks of Saurashtra are associated with picrites and ankaramites, andesites, dacites and rhyolites, and alkaline rocks including essexites, nepheline syenites, trachytes and lamprophyres (e.g. Sahu & Karim, 1993; Sethna & Javeri, 2000; Cucciniello *et al.* 2020; Sahoo *et al.* 2020). (ii) Saurashtra contains numerous plutonic complexes and ring dykes (Fig. 1), dominated by granophyre-microgranite (Sheth *et al.* 2011, 2022a; Cucciniello *et al.* 2019) and gabbro (Chatterjee, 1932; Banerjee *et al.* 2000). The Girnar Complex is dominantly of gabbro and diorite (Mathur *et al.* 1926; Cucciniello *et al.* 2022; Halder *et al.* 2023).

2.b. Topography and structure-controlled geomorphology

Much of the study area (~7,000 km^2, Figs. 1, 2) is topographically flat. Figure 3 shows the southwestern ~20% of this area, which is relatively rugged and where we have made particularly detailed field observations and sampling. All GPS-based coordinates of outcrops and their elevations (in metres above mean sea level) reported in this paper (Supplementary Table S1) have an uncertainty of ±3 m. All topographic features and localities mentioned are marked in Figs. 1–3, and numbers refer to both samples and outcrops.

https://doi.org/10.1017/S0016756823000432 Published online by Cambridge University Press

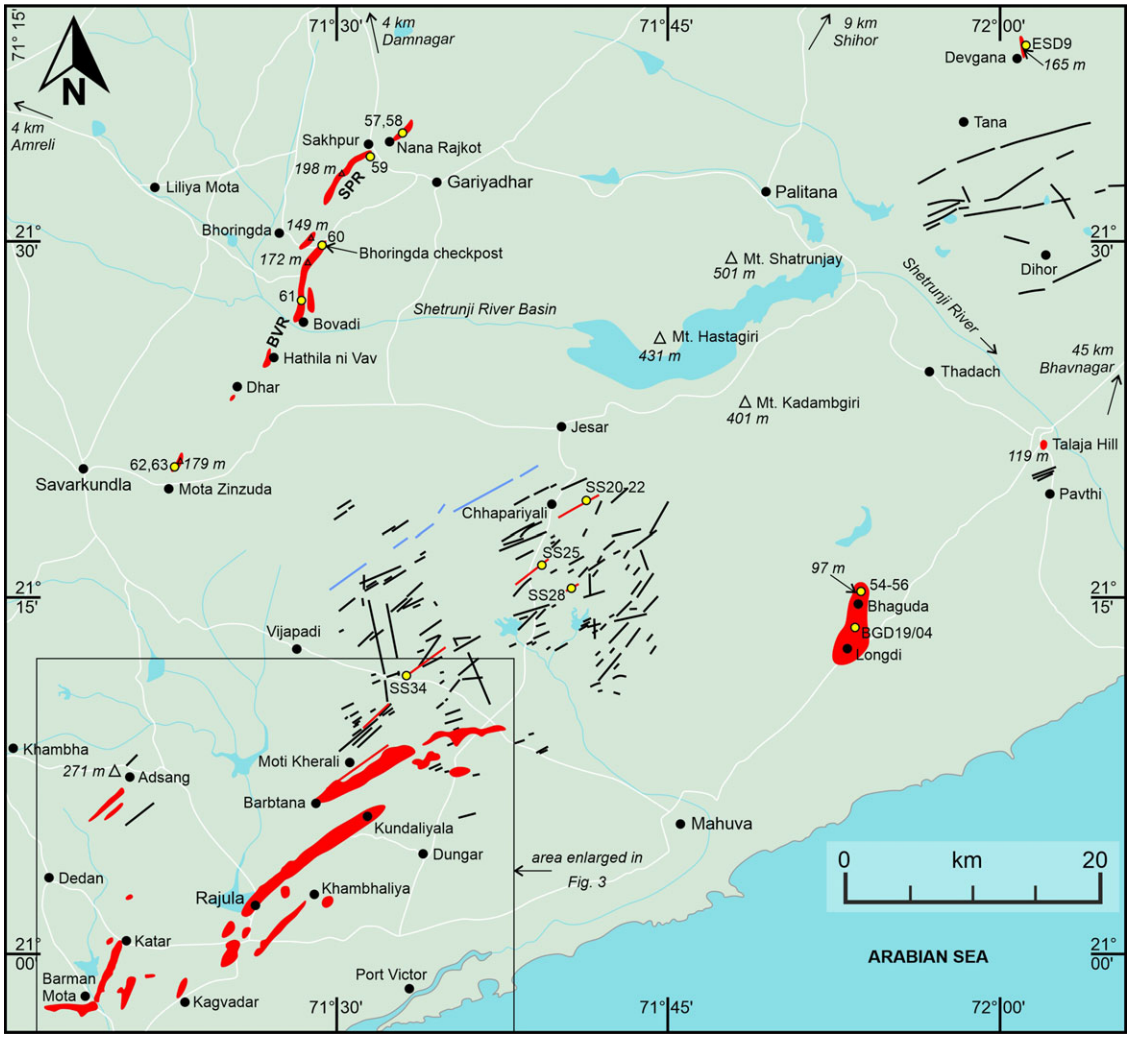

Figure 2. (Colour online) Geological map of the entire area of the present study shown in Fig. 1, showing topographic and geological features, localities mentioned in the text and sample locations. Light blue lines and areas are water bodies, and white lines are roads. Transparent open triangles represent significant elevations (italicized numbers, in metres above mean sea level) in an otherwise low-lying and flat landscape. Linear ridges of silicic volcanic rocks (e.g. Misra, 1976, 1981, 1999; Kshirsagar *et al.* 2012) are shown in red. Samples collected from them are indicated by yellow dots with numbers (without the prefix "RJ21" for avoiding cluttering), and ESD9 is from Kshirsagar *et al.* (2012). SPR and BVR are the Sakhpur and Bovadi ridges, respectively (see text). The pale green background is terrain composed of basaltic lava flows, forming flat areas, mountains or numerous structural ridges, which are not specially indicated. Short black and red lines are mafic dykes and silicic dykes, respectively, and the blue line is an andesite dyke. The prominent dyke cluster in the central part of the map is the Southeastern Saurashtra dyke swarm (Cucciniello *et al.* 2020); numbers with the prefix 'SS' represent silicic dykes analysed by them for geochemistry). The southwestern part (box shown in Fig. 2) of the entire study area, which has been studied and sampled in particular detail, is shown enlarged in Fig. 3.

The area consists of vast plains of basalts and alluvium, traversed by long linear rocky ridges. The volcanic rocks forming the ridges (either basaltic lava flows or basalts overlain by silicic units) dip gently southeast (12–16°). The ridges are, therefore, cuestas with asymmetrical cross-profiles, i.e., with long gentle dip slopes to the east or southeast and steep escarpments to the north and west (Misra, 1976, 1981, 1999; Ramasamy, 1995, Figs. 2–4). Good examples of cuestas of basalt are found at Vavdi (Fig. 4a) and Adsang (Fig. 4b). Around Hanumanpura just west of our study area (Fig. 3), steep (~45°) structural dips of the basalts have produced hogbacks (Fig. 4c). The basalts are dominantly pāhoehoe flows (both small-scale compound flows and sheet lobes) and rarely 'a'ā flows (Sheth *et al.* 2022b).

Other cuestas in the study area are composed of gently SE-dipping basaltic lava flows overlain by silicic volcanics (rhyolites and dacites), and often reach substantial size; they are named here after the adjacent villages (Fig. 3). The Moti Kherali Ridge reaches a length of 15 km and relief of up to 150 m above the surrounding flat terrain (Fig. 4d). The Barman Mota Ridge and the nearby, parallel Khalsa Kanthariya Ridge (Fig. 4e) are 4.8 and 2.8 km long, respectively. The silicic units are everywhere younger than the basalts, and, even with their tops eroded away, are tens of metres thick and show well-developed columnar jointing (Fig. 4f). Exposed vertical sections of these ridges show no palaeosols or sedimentary interbeds between the basalts and the silicic volcanics, indicating a conformable relationship.

There are numerous other kilometres-long rocky ridges found in the area (Figs. 2, 3), composed of silicic tuff breccias. The area also contains many mafic dykes and several silicic dykes, which form erosion-resistant linear ridges (Figs. 2, 3; see also Chaurasia & Jain, 2002; Raj & Jain 2002), but these dyke ridges have much lower relief than the other two types.

https://doi.org/10.1017/S0016756823000432 Published online by Cambridge University Press

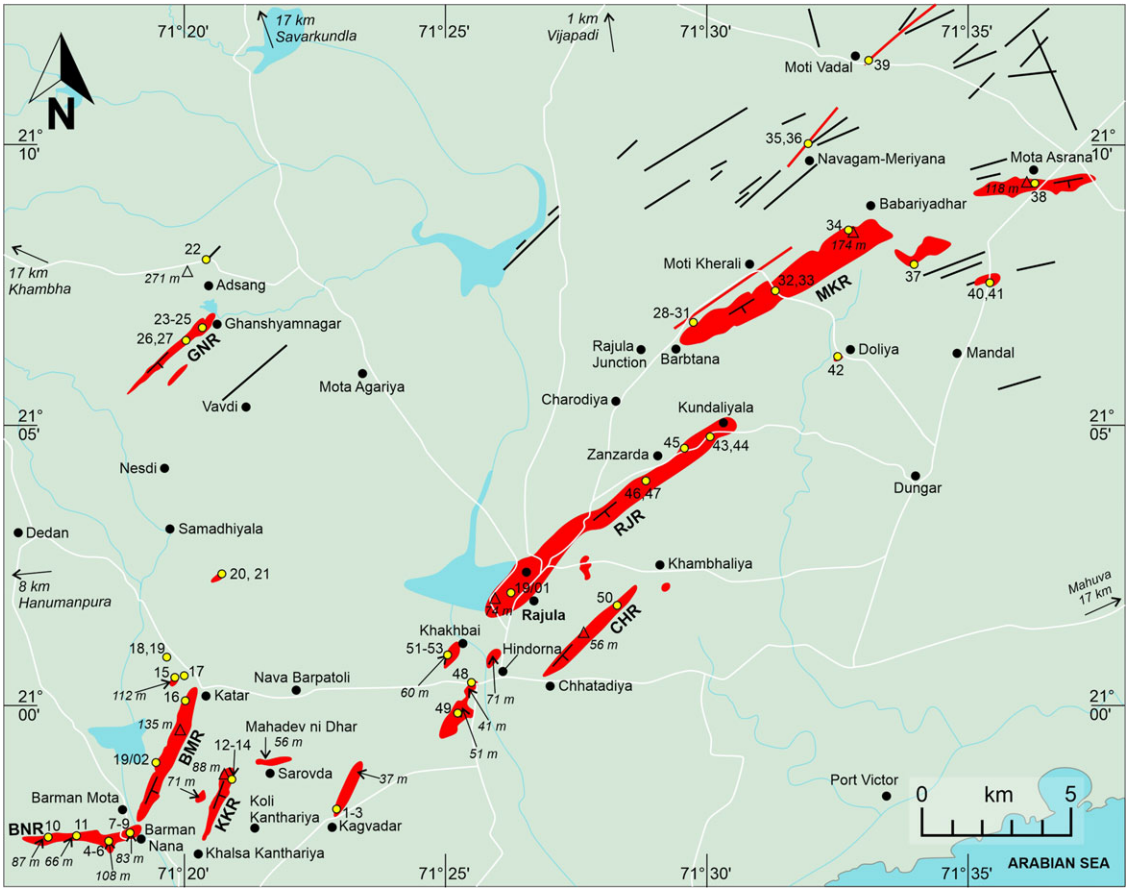

Figure 3. (Colour online) Geological map of the southwestern part of the study area shown in Figs. 1 and 2, showing topographic and geological features, localities mentioned in the text and sample locations (yellow dots with numbers). Light blue lines and areas are water bodies, and white lines are roads. Sample numbers are shown without the prefix RJ21 so as to avoid cluttering. As in Fig. 2, transparent open triangles show elevations in metres above mean sea level (italicized numbers). Linear ridges of silicic volcanic rocks are shown in red, and these include structural ridges of rheomorphic rhyolites and dacites shown with strike-dip symbols; the structural dips are everywhere towards the southeast. The main ones are Moti Kherali Ridge (MKR), Rajula Ridge (RJR), Barman Mota Ridge (BMR), Khalsa Kanthariya Ridge (KKR), Ghanshyamnagar Ridge (GNR) and Chhatadiya Ridge (CHR). Silicic tuff breccia ridges are Barman Nana Ridge (BNR) and Mahadev ni Dhar. The pale green background is terrain composed of basaltic lava flows and the many long linear structural ridges of the basalts, parallel to the silicic structural ridges, are not shown. Note, from west to east, a gradual and systematic change in the strike orientations of the structural ridges, from NNE-SSW through NE-SW to ENE-WSW. Black and red lines are mafic and silicic dykes, respectively.

2.c. Rheomorphic rhyolites and dacites

The silicic volcanics forming the cuestas are rhyolites and dacites as determined from prior petrographic and geochemical work (Chatterjee & Bhattacharji, 2001, 2004; Kshirsagar *et al.* 2012; Basu *et al.* 2020; Supplementary Table S2). The Rajula rhyolite, golden brown on weathered faces and, therefore, a popular building stone (Fig. 5a), is light grey on fresh surfaces, with small phenocrysts of white alkali feldspars. The light grey dacite capping the Barman Mota and Khalsa Kanthariya ridges is also feldspar-phyric.

A pervasive subhorizontal flow-banding is the prominent rheomorphic deformation feature observed in the Rajula rhyolite and the Barman Mota and Khalsa Kanthariya dacites (Fig. 5a, b). The rhyolite near Katar shows flow bands and folds (Fig. 5c, d). Other rhyolites show millimetre-scale flow banding (Fig. 5e, f). Flow banding is here taken as S_{0-1} and represents the transposition of the depositional fabric S_0 (typically unidentifiable in our rocks) during flow (D_1 rheomorphic deformation) (e.g. Andrews & Branney, 2011). The S_{0-1} bands have been rheomorphically deformed to produce folds of many different geometries, sizes and generations. These include F_1 open to tight folds (Fig. 5c–e, g), asymmetrical folds (Fig. 5f), isoclinal folds (Fig. 5h) and complex folds (Fig. 5i). Some fold limbs show highly stretched vesicles (Fig. 5d), whereas exposed fold surfaces show a well-defined elongation lineation L_1 (Fig. 5e). Refolding of F_1 tight to isoclinal folds by gentle to open F_2 folds is common (Fig. 5h).

The best exposures of rheomorphic deformation are located 1.5 km southeast of Moti Kherali village on the road to Doliya (Figs. 3, 6). The light grey rhyolite, with phenocrysts of white alkali feldspars and smoky quartz, shows prominent flow banding (Fig. 6a). There are F_1 tight to isoclinal folds (Fig. 6b–d) and sheath folds (Fig. 6e), and stretched and boudinaged flow bands (Fig. 6f). Single outcrops at this site show a range of F_1 fold geometries from symmetrical to asymmetrical and open to isoclinal, and fold orientations from subvertical to recumbent and inclined (Fig. 6g). Gentle to open F_2 folds reaching sizes of tens of metres are seen to refold the F_1 tight to isoclinal folds (Fig. 6b, g). This easily accessible site is an excellent potential geosite for its exquisite rheomorphic deformation features in rhyolite.

We observed the basal parts of the rheomorphic silicic eruptive units overlying basalt at many locations and generally found no autobreccias (e.g., Figs. 4d–f, 5b, c). However, at the northern end of the Khalsa Kanthariya Ridge, a well-developed basal autobreccia of dacite overlies a columnar-jointed basaltic sheet lobe in an

https://doi.org/10.1017/S0016756823000432 Published online by Cambridge University Press

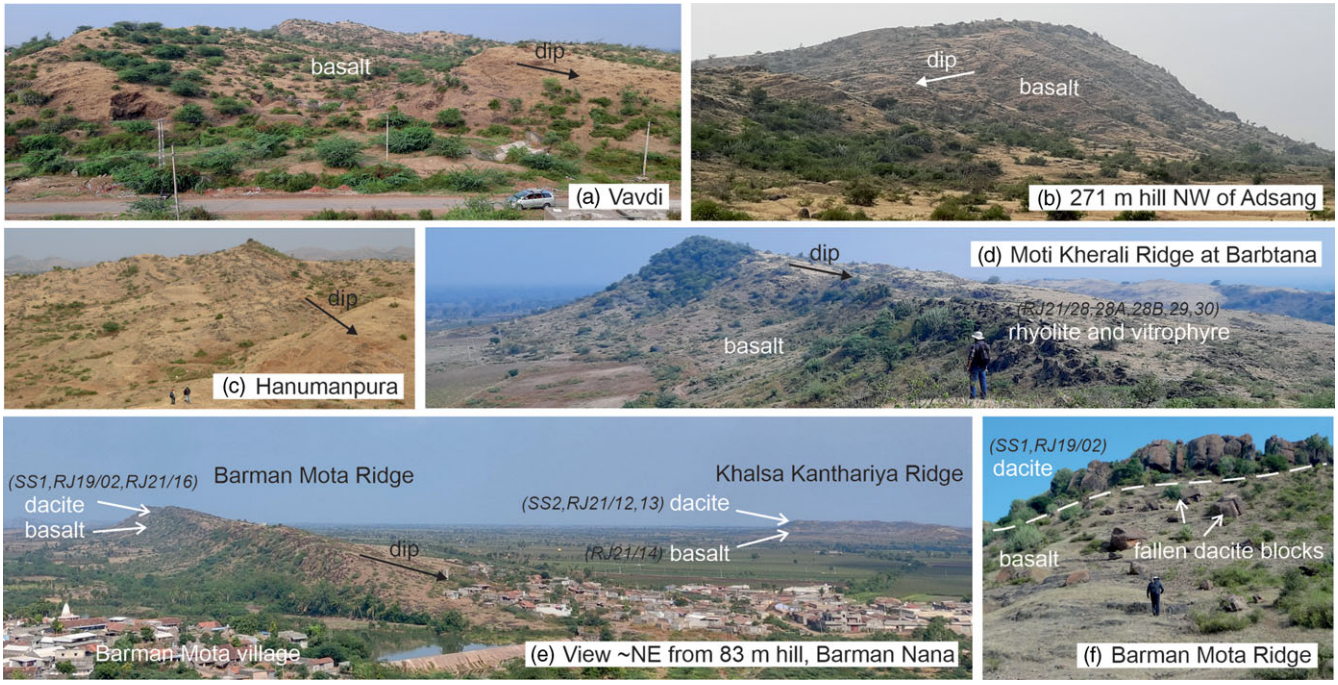

Figure 4. (Colour online) Photographs showing the typical landscape of the study area and field relationships between basaltic lava flows and silicic eruptive units. All localities are marked in Figs. 2 and 3. In this and subsequent figures, samples collected in previous studies ('SSxx', Kshirsagar *et al.* 2012 and Cucciniello *et al.* 2020, and 'ESD, Kshirsagar *et al.* 2012) and in the present work are indicated by numbers in italics, and their locations (GPS-based coordinates) are provided in the Supplementary Table S1. (a) Basalt cuestas with southeasterly dip slopes at Vavdi. Car provides a scale. (b) Prominent 271 m basalt hill near Adsang. Relief is ~100 m. (c) Hogback of steeply dipping basaltic lava flows at Hanumanpura. Persons for scale. (d) The southwestern end of the ENE-WSW-trending Moti Kherali cuesta ridge at Barbtana, with various rhyolitic facies overlying basalt. Person for scale. (e) The Barman Mota and Khalsa Kanthariya cuesta ridges, with gently SE-dipping dacites overlying mafic lava flows (Misra, 1976; Kshirsagar *et al.* 2012; Sheikh *et al.* 2020a). (f) View of the escarpment face in the southern part of the Barman Mota Ridge, showing columnar-jointed dacite overlying a highly weathered mafic lava flow (mentioned by Misra (1976) as a trachyandesite). Person for scale.

abandoned quarry pit (Fig. 7a–d). This clast-supported autobreccia is up to a few metres in exposed thickness and contains large (many > 10 cm) angular fragments of vesicular dacite in a dark, glass-rich matrix (Fig. 7b, c). A vertical, centimetre-thick rhyolitic dykelet with sharp margins was seen intruding the autobreccia (Fig. 7d).

The 71 m, NNE-SSW-elongated hillock located between the Barman Mota and Khalsa Kanthariya ridges (Fig. 7e), probably constituting their extension, is made up of clasts of vesicular and flow-banded rhyolite or dacite (Fig. 7f). Some large flow bands in between the clasts can be traced over several metres, and the base of the breccia is not exposed. The top of the 71 m Hindorna Hill just south of Rajula town is composed of rheomorphic rhyolite, but breccia is found below this (Fig. 7g). Southwest of Hindorna, the top of the 51 m hillock, shows possible autobreccia (Fig. 7h), whereas the 41 m hillock shows blocks of breccia *within* rheomorphic rhyolite (Fig. 7i).

2.d. Pitchstones and vitrophyres

Pitchstone is silicic volcanic glass with much more crystalline material and H_2O (up to 6 wt.%) than obsidian (<1 wt.% H_2O) and, therefore, has a waxy or resinous lustre, unlike the vitreous lustre and characteristic conchoidal fracture of obsidian (Hatch *et al.* 1983). Vitrophyre is silicic glass with abundant phenocrysts.

Bands of silicic glass are encountered at several places and are often surprisingly fresh (Misra, 1981, 1999; Banerjee, 1998). An outcrop near Kagvadar shows decimetre-scale bands of fresh pitchstone (locally obsidian) and altered, spherulitic pitchstone (Fig. 8a, b). Kshirsagar *et al.* (2012) reported a nearby pitchstone outcrop with decimetre-scale subhorizontal banding, some bands showing a profuse development of spherulites 3–4 mm in diameter (Fig. 8c, d).

The other silicic glasses in the area are all vitrophyres and are typically overlain by lava-like rhyolites, as at Khakhbai Hill, Bhaguda Hill, the Moti Kherali Ridge at Barbtana and a location 3 km north of Mandal. Columnar-jointed vitrophyre forms a small exposure at Doliya, within a large flat, cultivated area without rock outcrops (Fig. 8e). In the Bhaguda Hill, vitrophyre overlies eutaxitic ignimbrite and green tuff and is overlain by brown lava-like rhyolite (see also Sheikh *et al.* 2020a). In the Moti Kherali Ridge at Barbtana, vitrophyre is overlain by rheomorphic, lava-like red rhyolite, and patches of fresh vitrophyre (Fig. 8b) are found within the rhyolite. In the Rajula Ridge near Kundaliyala, vitrophyre *overlies* rhyolite (Fig. 8f). Vitrophyric portions are found in the southern margin of a NE-SW-trending rhyolitic dyke at Navagam-Meriyana.

2.e. Tuffs and ignimbrites

Krishnamacharlu (1974) described three distinct units of ignimbrite, 3–10 m thick and with a 'fluxion' structure, overlying pitchstone 'about 1 km northeast of Rajula'. His given coordinates of N 21° 2' and E 71° 29' plot a few kilometres to the east within cultivated fields. In the Moti Kherali Ridge at Barbtana, altered vitrophyre overlies lapilli tuff, which grades laterally into eutaxitic ignimbrite (Fig. 8g). This may be the site described by Krishnamacharlu (1974), actually located 2 km northeast of Rajula Junction railway station, though we have not found the three ignimbrite units he described.

https://doi.org/10.1017/S0016756823000432 Published online by Cambridge University Press

Figure 5. (Colour online) Rheomorphic rhyolites and dacites of the study area. (a) Quarry in the Rajula rhyolite, person for scale. (b) Dacite forming the northern parts of the Barman Mota Ridge, person for scale. (c) Rhyolite ~2 km northwest of Katar on the road to Dedan. (d) Close-up of the fold seen in the previous panel. Arrows indicate stretched vesicles. Vertical section view, hammer is 28 cm long. (e) Upright fold in millimetre-scale flow-banded rhyolite, with L_1 lineation (probably a stretching/elongation lineation) on the fold surfaces. Location ~2 km southeast of Samadhiyala. (f) Hand-held chip of rhyolite forming the 41 m hillock southwest of Hindorna. (g) Large open F_1 fold (traced by the yellow line) in brown rhyolite near the summit of Bhaguda Hill. (h) Superposed folding in dacite in the northern part of the Khalsa Kanthariya Ridge, with F_2 refolding of F_1 folds. (i) Intense and complex flow-folding in rhyolite of 41 m hillock southwest of Hindorna. Subhorizontal view of inclined outcrop face, hammer 33 cm long. See Sheikh *et al.* (2020a) for additional photographs.

Eutaxitic ignimbrite has also been described from Bhaguda Hill (Sheikh *et al.* 2020a). The hill exposes brown lava-like rhyolite at the 97 m summit (Fig. 5g), underlain successively by vitrophyre, eutaxitic ignimbrite (Fig. 8h, i) and massive green tuff. The vitrophyre and green tuff continue southwards, and the latter forms extensive outcrops between Bhaguda and Longdi.

2.f. Spherulites and lithophysae

Spherulites are composed of radiating microscopic fibres of alkali feldspar and quartz and form due to heterogeneous nucleation in highly supercooled silicic melts or by devitrification of glass (e.g. Cross, 1891; Marshall, 1961; Lofgren, 1971; Breitkreuz, 2013). Their spherical shape may be due to the isotropic physical properties of the host melt or glass, implying the absence of any preferred direction of growth, or to non-crystallographic branching of mineral fibres as a space-filling mechanism (Vernon, 2018). Lithophysae ('stone bubbles') have an exterior (sometimes concentric shells) of fine quartz and feldspar and internal cavities left by escaping gas, and when filled by secondary silica, these are termed thundereggs (Tyrrell, 1926; Breitkreuz, 2013).

The few notable spherulite occurrences in the area were mentioned above (see also Kshirsagar *et al.* 2012). Lithophysae are much more common, for example, in the Khalsa Kanthariya and Moti Kherali Ridges (Fig. 9a, b). Profuse local development of hundreds of lithophysae, each a few centimetres in size, is observed in the rheomorphic rhyolite just southwest of Ghanshyamnagar (Fig. 9c), and at the top of Khakhbai Hill (Fig. 9d) where individual lithophysae are up to 15 cm across. Lithophysae are also found within the fresh pitchstone of Kagvadar (Fig. 9e, f).

Development of lithophysae on an extraordinary scale is observed about halfway between Bhaguda and Longdi, where a gently rolling plain of altered green tuff exposes tens of thousands of lithophysae ranging in size from <1 mm to ~10 cm or so, most being a few centimetres in size (Fig. 9g–i). Besides the common single lithophysae, there are twins, triplets and even quadruplets (see photos in Misra, 1999; Kshirsagar *et al.* 2012; Sheikh *et al.* 2020a).

https://doi.org/10.1017/S0016756823000432 Published online by Cambridge University Press

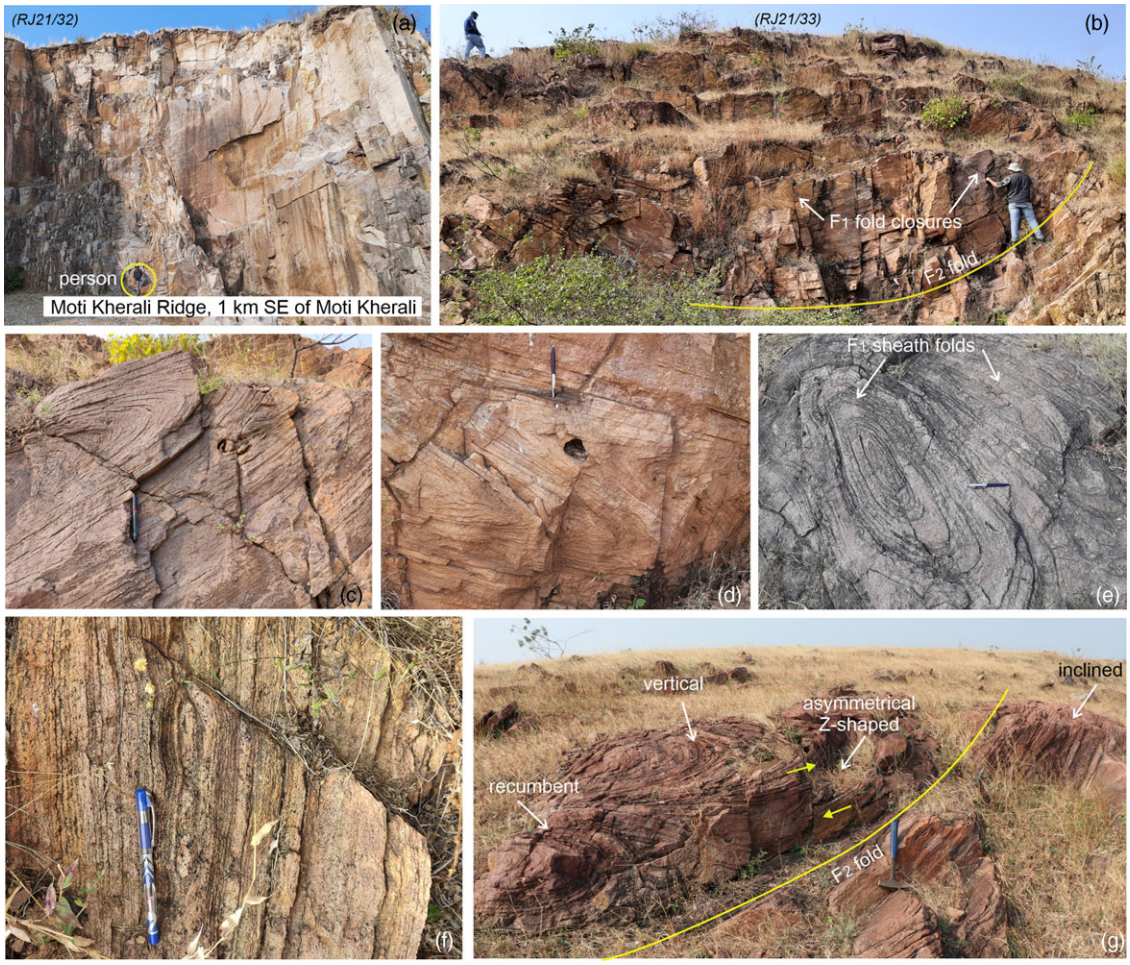

Figure 6. (Colour online) Rheomorphic deformation features in the rhyolite of the Moti Kherali Ridge, exposed ~1.5 km southeast of Moti Kherali village, an excellent potential geosite at N 21° 07' 19.7", E 71° 31' 20.4", el. 77 m. (a) Abandoned quarry exposing flow banding, person (encircled) for scale. (b) Large F_1 folds refolded by larger-scale F_2 folds. (c, d) Vertical section views of tight to isoclinal F_1 folds with inclined axial planes. Pen in each is 14 cm long. (e) Two adjacent, stretched F_1 sheath folds. Oblique view of subhorizontal ground surface, pen 15 cm long. (f) Boudinage of a flow band just next to the 15 cm long, vertical section. (g) Folds of several types, orientations and generations, the hallmark of rheomorphic deformation, seen on a subhorizontal ground surface. Pair of short yellow arrows indicates a dextral sense of shear during folding. Hammer is 33 cm long and vertical.

In addition to the megascopic examples of spherulites and lithophysae, microscopic ones are found in many of the rock units and are described below.

2.g. Tuff breccias

Like the rheomorphic rhyolites and dacites, the silicic tuff breccias form long linear ridges (or distinctly aligned hills) that rise 70–80 m from the basaltic or alluvial plains and often extend for many kilometres. However, unlike the case with the rheomorphic rhyolites and dacites, the tuff breccias are not observed in stratigraphic contact with the other rock types.

In the alluvial plain of the Shetrunji River (Fig. 2), alignments of tuff breccia hills appear to define two ridges, each slightly curved but with an overall NNE-SSW trend. The western ridge, which we term the Sakhpur Ridge, runs from Nana Rajkot through Sakhpur to the 149 m hill just east of Bhoringda, a distance of some 14 km. The eastern ridge, termed here the Bovadi Ridge, runs from Bhoringda police checkpost through Bovadi, continues through Hathila ni Vav and Dhar and terminates at Mota Zinzuda, a total distance of some 22 km. These lengths are minimum lengths as the tuff breccias of either ridge may continue further under the alluvium (Fig. 2). At every location visited in the Sakhpur Ridge (Fig. 10a–d) and the Bovadi Ridge (Fig. 10e–i), the tuff breccias are entirely massive, lacking bedding, size sorting or grading and any preferred orientations of clasts, and are commonly clast-supported. The clasts are many centimetres in size and typically angular. The tuff breccias are extensively silicified and ferruginized.

Two isolated hills, located at Talaja and Devgana in the eastern and northeastern parts of the area, respectively (Fig. 2), are composed of similar tuff breccias. Talaja Hill (119 m, Fig. 11a) is a poorly maintained archaeological and religious site, with rock-cut caves in the western side composed of pumice and tuff breccias. The pumice is characteristically highly vesicular (Fig. 11b, c). Metre-size and smaller blocks of pale grey tuff within an ash-size matrix, resembling fault breccia, are exposed within one of the caves (Fig. 11d), and bedded and faulted ash beds are found within another cave (Fig. 11e). The higher, eastern side of the hill is composed mainly of tuff breccias (Fig. 11f). The Devgana Ridge (140 m) is a N-S-trending linear ridge composed of altered silicic tuff breccias, which as elsewhere are massive and unsorted (Fig. 11g, h).

https://doi.org/10.1017/S0016756823000432 Published online by Cambridge University Press

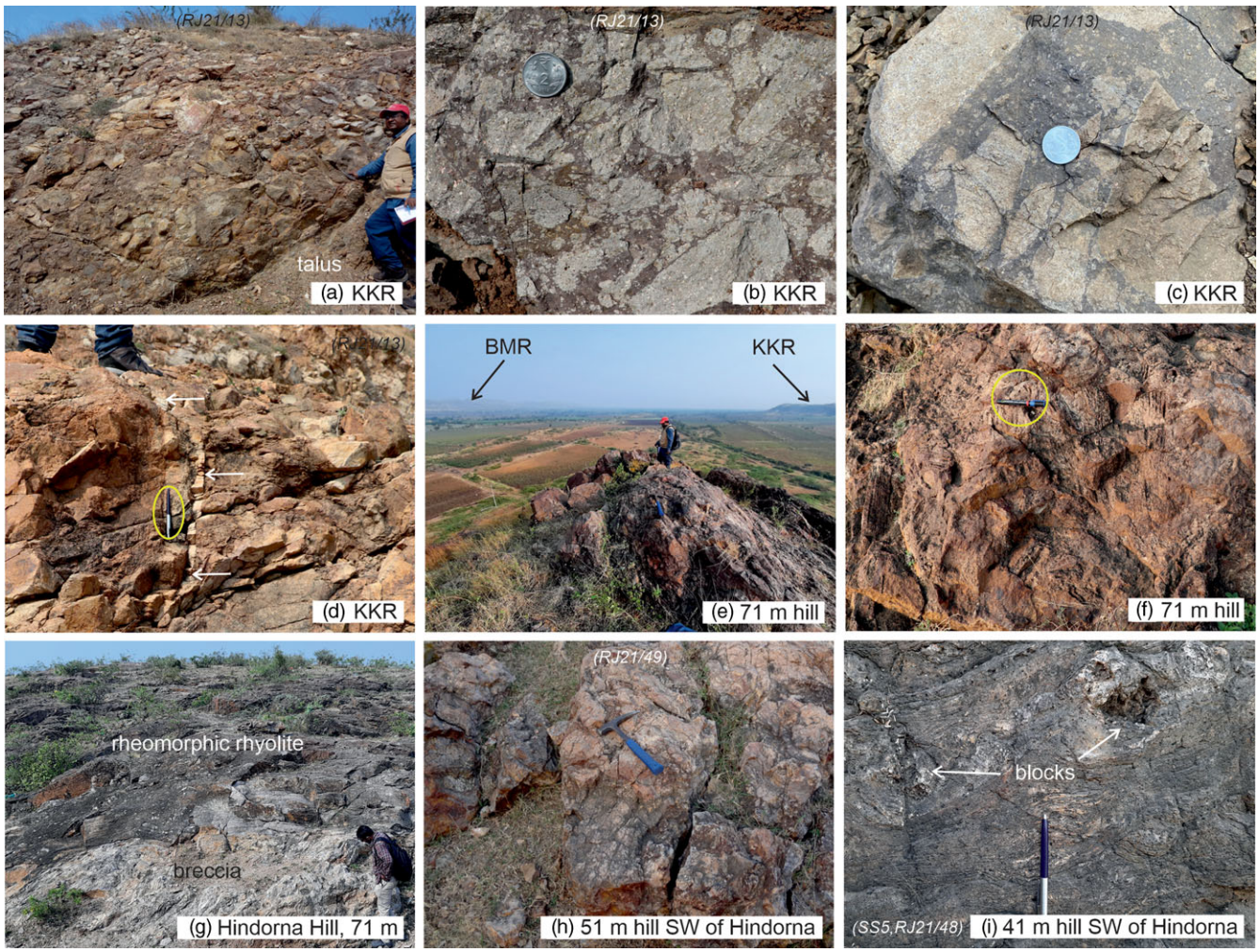

Figure 7. (Colour online) Autobreccias in the rhyolites and dacites of the study area. (a) Basal autobreccia of dacite at the northern end of the Khalsa Kanthariya Ridge (KKR). (b, c) Close-up views of the dacite basal autobreccia in *a*, with 2.5 cm wide coins for scale. (d) A thin rhyolitic dykelet with sharp margins (white arrows) within the basal autobreccia. Vertical section view, with 15 cm long pen (within ellipse). The dykelet cannot be traced in plan view beyond the person's feet. (e) Autobreccia of flow-banded dacite or rhyolite forming the 71 m hillock between the dacite-capped Barman Mota Ridge (BMR) and the KKR. Person for scale. (f) Close-up of the autobreccia forming the 71 m hillock; note flow banding, vesicles and stretched vesicles. Pen (encircled) is 14 cm long. (g) Probable autobreccia below intensely rheomorphic rhyolite at the top of the 71 m Hindorna Hill, person for scale. (h) Probable autobreccia exposed on the top of the 51 m rhyolite hillock southwest of Hindorna. Hammer is 33 cm long. (i) Irregularly shaped rhyolite blocks within strongly rheomorphic rhyolite forming the 41 m hillock southwest of Hindorna.

Notable silicic tuff breccias are also found in the southwestern corner of the area (Figs. 2, 3). They form the 4 km-long Barman Nana Ridge (Fig. 12a) and the low (56 m) mound of Mahadev ni Dhar (Fig. 3). These E-W-trending tuff breccia ridges are notably oblique (120°) to the NNE-SSW-trending Barman Mota and Khalsa Kanthariya ridges of rheomorphic dacite (Figs. 3, 12a). Though the tuff breccias and the rheomorphic dacites are nowhere observed in contact, the tuff breccias appear to be younger. As elsewhere (Figs. 10, 11), the tuff breccias forming the Barman Nana Ridge and Mahadev ni Dhar mound are massive and lack any clast fabric. They range from matrix-supported to clast-supported, with pervasive silicification and ferruginization (Fig. 12b–g). One additional feature observed in the 108 m hill in the Barman Nana Ridge is that its basal part shows unconsolidated, massive, greyish white ashes underlying the tuff breccias (Fig. 12c), mentioned by Misra (1976) as altered andesitic tuffs. At places, they show large-scale Liesegang rings and are intruded by a set of subvertical to steeply dipping rhyolitic dykes with strikes between N250° and N215° (Fig. 12c).

2.h. Mafic and silicic dykes

Numerous mafic and silicic dykes occur in the area (see also Sethna *et al.* 2001; Cucciniello *et al.* 2020) and are generally seen to intrude the basaltic lava flows. No dyke was observed to pass into (feed) a volcanic unit, though some of the dykes might have fed higher stratigraphic levels of the volcanic sequence now lost by erosion.

The prominent dyke cluster in the central part of Fig. 2 is the Southeastern Saurashtra dyke swarm as mapped by Cucciniello *et al.* (2020) using the then-available Survey of India 1:50,000 topographic sheets. New satellite imagery such as *Google Earth* shows that several of the dykes are longer than shown. This dyke swarm differs from the exclusively mafic Eastern Saurashtra, Central Saurashtra and circum-Girnar dyke swarms (Fig. 1, Cucciniello *et al.* 2022 and references therein) in containing silicic members. It is also intriguing that whereas several strike directions are represented in the swarm (mainly NE-SW, ENE-WSW and NNW-SSE), the silicic dykes all strike NE-SW. Cucciniello *et al.* (2020) studied many dykes of this swarm for mineral chemistry and whole-rock geochemistry (including Sr-Nd isotopes) and

https://doi.org/10.1017/S0016756823000432 Published online by Cambridge University Press

Figure 8. (Colour online) Pitchstones, vitrophyres and eutaxitic ignimbrites of the study area. (a) Fresh, black pitchstone and altered spherulitic pitchstone at Kagvadar. (b) Close-up view of hand specimens of the fresh Kagvadar pitchstone shown in *a* and the vitrophyre found in the Moti Kherali Ridge at Barbtana. Coin is 2 cm wide. (c, d) Spherulitic pitchstone banded on a large scale at Kagvadar; outcrop described by Kshirsagar *et al.* (2012). (e) Small vitrophyre outcrop at Doliya. (f) Vitrophyre (yellow-weathering, columnar) above brown rhyolite, south of Kundaliyala. (g) Close-up view of eutaxitic ignimbrite in the Moti Kherali Ridge (MKR) at Barbtana, coin 2.5 cm wide. (h, i) Eutaxitic ignimbrites in the Bhaguda Hill; 2.5 cm wide coin and hand for scale. See also Sheikh *et al.* (2020a).

found substantial input from Precambrian basement crust, especially the silicic dykes.

Some of the dykes in the area are multiple and were produced by repeated magma injections. A good example is a mafic dyke with six columnar-jointed rows exposed ~1 km north of Adsang (Fig. 13a). The dyke intrudes an altered basaltic lava flow, strikes N30° and dips 75° NW, and its six columnar rows suggest three or more separate magma injections. The silicic dykes appear to represent single magma injections. Examples include the N57°-trending, extensively spherulitic Chhapariyali rhyolite dyke with vitrophyric portions (Fig. 13b, Sheikh *et al.* 2023). Another is a N40°-striking rhyolitic dyke at Navagam-Meriyana, with sub-vertical flow banding and margins that are vitrophyric at places (Fig. 13c, d). Both these dykes intrude the basaltic lava flows.

There are also a few dykes intruding the tuff breccia ridges. Rhyolitic dykes with strikes ranging from NNE-SSW to ENE-WSW intrude the tuffs and breccias of the Barman Nana Ridge (Figs. 12c, 13e). A dolerite dyke striking N320° and dipping 42° NE intrudes the tuff breccia of the Devgana Ridge (Fig. 13f). Because the tuff breccias are younger than the basaltic lava flows and the rheomorphic rhyolites and dacites, the dykes intruding the tuff breccias constitute the youngest magmatic phase in the area.

2.i. Mafic enclaves

Cucciniello *et al.* (2020) and Sheikh *et al.* (2023) have noted that mafic enclaves are a common feature of the silicic members of the Southeastern Saurashtra dyke swarm. The mafic enclaves range in size from <1 mm to 30 cm and have rounded and cuspate but typically sharp margins with the host rhyolite (Fig. 13g). The rheomorphic rhyolite of the Moti Kherali Ridge at Barbtana village and the silicic tuff breccia forming the 83 m hill in the Barman Nana Ridge also contain a few mafic enclaves (Fig. 13h, i).

3. Petrography and textures

Textures of volcanic rocks observed under the microscope provide valuable clues to their origin and emplacement (e.g. McPhie *et al.* 1993; Vernon, 2018). We therefore carried out petrographic and textural studies of the various silicic rocks and present our observations below.

https://doi.org/10.1017/S0016756823000432 Published online by Cambridge University Press

Figure 9. (Colour online) Lithophysae in the silicic rocks of the study area. (a) Small lithophysae exposed in plan in the Khalsa Kanthariya Ridge (KKR) dacite. Pen cap is 3 cm long. (b) Cluster of many small intergrown lithophysae in the rhyolite of Moti Kherali Ridge (MKR) at Barbtana. Coin at photo centre is 2.5 cm wide. (c) Local bonanza of lithophysae in the Ghanshyamnagar Ridge (GNR) at Ghanshyamnagar. Vertical section view, hammer 33 cm long. (d) A cluster of lithophysae in the rhyolite of Khakhbai Hill. Plan view, hand-held GPS for scale. (e) Vertical section through the fresh Kagvadar pitchstone containing many lithophysae. Hammer is 28 cm long. (f) Close-up of a single lithophysa in the Kagvadar pitchstone shown in (e), with a 2.7 cm coin for scale. (g) Lithophysae jackpot about halfway between Bhaguda and Longdi. Some 15 lithophysae (indicated by white and black arrows) are seen within weathered pale green tuff. Oblique plan view; 14 cm long pen (encircled) is vertical. (h) Close-up of a lithophysa at the location in *g*, showing apparent budding (white arrow). Coin is 2.7 cm wide. (i) Plan view of a collection of lithophysae made within minutes at the location in (g, h). See Misra (1999), Kshirsagar *et al.* (2012) and Sheikh *et al.* (2020a) for additional photographs.

3.a. Rheomorphic rhyolites and dacites

The rheomorphic rhyolites and dacites are crystal-rich, with the phenocrysts dominantly of quartz and alkali feldspar (Fig. 14a–g). We use the term phenocryst in a purely textural sense, without genetic connotations, for easily identifiable crystals much larger than the groundmass (Iddings, 1892; Zellmer, 2021). The quartz phenocrysts are angular to rounded, commonly traversed by fractures (Fig. 14b–g), and sometimes embayed (Fig. 14f, g). Alkali feldspar phenocrysts are euhedral to subhedral and lath-shaped (Fig. 14a–c). Both minerals form phenocrysts in the Bhaguda Hill summit rhyolite (Kshirsagar *et al.* 2012).

Dacites of the Barman Mota and Khalsa Kanthariya ridges and the 112 m hill, and the Rajula quarry rhyolite show glomerocrysts of feldspars and olivine (Fig. 14a, c), sometimes with minor orthopyroxene, in decreasing order of abundance. Glomerocrysts of plagioclase several millimetres in size are abundant in the rhyolite exposed 3 km north of Mandal (Fig. 14h); the constituent crystals show large numbers of melt inclusions, and many crystals show oscillatory zoning in cross-polarized light. The Bhaguda Hill summit rhyolite also shows such plagioclase glomerocrysts, and some crystals display bent twin lamellae (Fig. 14i), suggesting some deformation of the crystal-bearing magma.

Groundmasses of the various rocks are fine and microcrystalline, composed of quartz and alkali feldspar. A micropoikilitic or 'snowflake' texture (Anderson Jr., 1969; McPhie *et al.* 1993) is common, in which anhedral crystals of quartz or alkali feldspar contain numerous microlites of feldspar (Fig. 14a, c, f, i). A well-developed flow banding defined by aligned alkali feldspar microlites is seen in the dacite of Khalsa Kanthariya Ridge (Fig. 14b). In the rhyolite near Samadhiyala, phenocrysts of quartz are surrounded by glass-rich bands (Fig. 14d). In the rhyolite of Moti Kherali Ridge at Barbtana, numerous spherulites are seen to have nucleated on the corners of quartz phenocrysts, and others in the groundmass between the phenocrysts (Fig. 14e), whereas the rhyolite 3 km north of Mandal shows tiny lithophysae. Vitroclasts (glass shards and pumice fragments) are absent in all rocks examined.

https://doi.org/10.1017/S0016756823000432 Published online by Cambridge University Press

Figure 10. (Colour online) Rhyolitic tuff breccia ridges and outcrops in the Shetrunji River alluvial plain (northwestern quadrant of Fig. 2). (a) Tuff breccia outcrop at the Khodiyar temple near Nana Rajkot village, forming the exposed northern end of the Sakhpur Ridge which is visible in the distance. View is towards the southwest. (b) Close-up of the tuff breccia at Nana Rajkot. Coin is 2.7 cm wide. (c) Close-up of extensively ferruginized tuff breccia at Sakhpur, coin 2.7 cm wide. (d) Lapilli tuff near Bhoringda, coin 2.5 cm wide. (e, f) Tuff breccias at Bhoringda police checkpost, the northern exposed end of the Bovadi Ridge. Hammer is 33 cm long and coin 2.5 cm wide. Note extensive silicification. (g) Tuff breccia at Hathila ni Vav, pen 14 cm long. (h, i) Tuff breccias in the hills with Khodiyar temples at Bovadi and at Mota Zinzuda; persons' feet provide a scale.

3.b. Pitchstones and vitrophyres

The fresh pitchstone of Kagvadar lacks phenocrysts and shows a few well-developed spherulites and lithophysae in a groundmass with spectacular acicular, feathery and fernlike growths of feldspar (Fig. 15a). The vitrophyres, as the name suggests, are crystal-rich with glassy groundmasses (Fig. 15b–i). Quartz is the most common phenocryst and typically forms rounded and fractured grains (Fig. 15b, e, f, i). The vitrophyre of the Moti Kherali Ridge at Barbtana shows some mafic enclaves (Fig. 15b) whose larger versions are seen in outcrop in the surrounding rheomorphic rhyolite (Fig. 13h).

A major petrographic feature of essentially all the vitrophyres are crystal aggregates or glomerocrysts of plagioclase and ferromagnesian minerals (most commonly orthopyroxene, with less clinopyroxene and olivine). Orthopyroxene is found, commonly with abundant plagioclase, in the vitrophyres at Barbtana, 3 km north of Mandal (Fig. 15c), Doliya (Fig. 15e), Zanzarda (Fig. 15f), Khakhbai Hill (Fig. 15g), Bhaguda Hill (Fig. 15h) and the Navagam-Meriyana dyke (Fig. 15i). Some plagioclase crystals contain many melt inclusions (Fig. 15c, g, h), and other crystals are evidently broken (Fig. 15e).

The glassy groundmasses of the vitrophyres often show a well-developed flow banding, defined by aligned microlites and crystallites of alkali feldspars and Fe-Ti oxides (Fig. 15b–d). The flow bands wrap around crystals and are often folded (Fig. 15c, d) and refolded (Fig. 15b). Darker and lighter flow bands reflect high and low densities of microlites and crystallites (including those of submicroscopic size); similar observations have been made at Osham Hill (Fig. 1), for example (Sheikh *et al.* 2020a; Naik *et al.* 2021). High-magnification examination reveals trains of hundreds of flow-sorted crystallites, many forming axiolitic arrangements, defining the flow bands (Fig. 15d). Numerous small spherulites are seen in some samples (Fig. 15f), and perlitic cracks are developed in different degrees in all samples.

In contrast to the many fresh vitrophyres illustrated above, vitrophyres from the Moti Kherali Ridge at Barbtana and Khakhbai Hill are altered (Fig. 16a, b) and provide good examples of 'false vitroclastic' textures produced by phyllosilicate alteration along perlitic cracks (Allen, 1988; McPhie *et al.* 1993, p. 22, their Fig. 15). The former vitrophyre shows large, embayed quartz phenocrysts in a glassy matrix traversed by a network of perlitic cracks. Alteration along the cracks has left polygonal to rounded areas between the

https://doi.org/10.1017/S0016756823000432 Published online by Cambridge University Press

Figure 11. (Colour online) Essential volcanological features of the Talaja Hill (119 m). (a) View of the hill with the rock-cut caves in the western side, composed of pumice blocks and tuff breccias, and the higher, eastern side, composed mainly of tuff breccias. White buildings are temples. (b) One of the caves carved in pumice. (c) Close-up of the pumice, coin 2.5 cm wide. (d) Blocks of pale grey tuff within an ash-size matrix in one of the caves. Vertical face, hammer 33 cm long. (e) Bedded and faulted ash beds within another cave. Vertical face, hammer 33 cm long. (f) Lapilli tuffs in the eastern side of the hill, exposed in the scarp seen in panel (a). Coin is 2.5 cm wide. (g) The N-S-trending Devgana Ridge. (h) Close-up of the Devgana Ridge rhyolitic tuff breccia. Visible part of hammer is ~62 cm long.

cracks that produce a false impression of blocky to cuspate glass shards in a vitric tuff (Fig. 16a). The latter vitrophyre has been altered along a very close-spaced network of perlitic cracks, and this has produced an impression of vitroclasts including the classical dark pumice fiamme in a eutaxitic ignimbrite (Fig. 16b). As with the rheomorphic rhyolites and dacites, vitroclasts are absent in all glasses examined.

3.c. Tuffs and ignimbrites

Rhyolitic tuff underlying lithophysae-rich rheomorphic rhyolite near Ghanshyamnagar (Fig. 9c) shows a dark microcrystalline matrix full of fine iron oxide grains and stretched and devitrified-recrystallized vitroclasts (Fig. 16c). Excellent vitroclastic textures are seen in the lapilli tuff overlying basalt in the Moti Kherali Ridge at Barbtana (Fig. 16d, e). This tuff shows an abundance of glass shards, pumice fragments and quartz crystals and can be described a crystal-vitric tuff. The glass shards are blocky, platy or cuspate bubble-wall shards (including Y-shaped shards). The pumice is fibrous or woody, owing to highly stretched vesicles, but pumice clasts do not show flattening. The eutaxitic ignimbrite of Bhaguda Hill shows pumice fiamme and quartz phenocrysts in a glassy matrix. The fiamme and matrix glass are pseudomorphed by clusters of dozens of tiny spherulites owing to devitrification (Fig. 16f).

4. Discussion

4.a. Effusive silicic volcanism

4.a.1. Rheomorphic rhyolites and dacites

The rheomorphic rhyolites and dacites always overlie basaltic lava flows without palaeosols or basalt-derived conglomerates in between, suggesting a conformable relationship and rapid volcanism without hiatuses. The absence of sedimentary interbeds and peperites indicates a subaerial setting for the eruptions.

Silicic lavas, and high-grade to extremely high-grade, lava-like ignimbrites both commonly contain rheomorphic deformation features (e.g., Christiansen & Lipman, 1966; Benson & Kittleman, 1968; Smith & Houston, 1994; Andrews & Branney, 2011; Bullock *et al.* 2018; Sheikh *et al.* 2020a, b; Naik *et al.* 2021). Thus,

https://doi.org/10.1017/S0016756823000432 Published online by Cambridge University Press

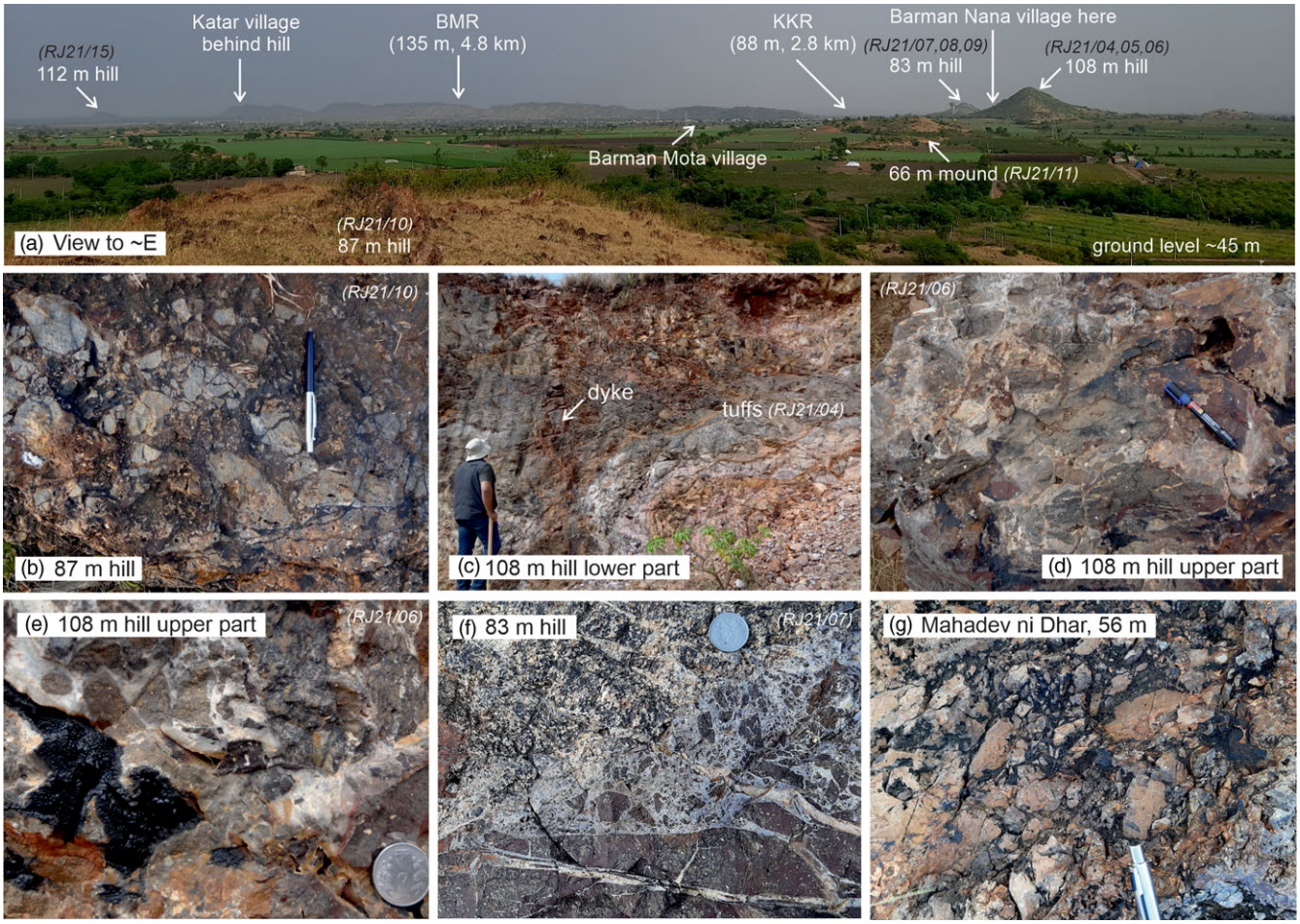

Figure 12. (Colour online) Rhyolitic tuff breccia hillocks and outcrops southwest of Rajula town (southwestern corners of Figs. 2, 3). (a) Panoramic view of the E-W-trending Barman Nana Ridge (consisting of the 87 m, 66 m, 108 m and 83 m hills), with the Barman Mota and Khalsa Kanthariya ridges of rheomorphic dacite (BMR, KKR) in the distance. The 112 m hill shown is composed of the same dacite. (b) Close-up of tuff breccia forming the 87 m hill, pen 15 cm long. (c) Soft, unbedded andesitic ashes forming the lower part of the 108 m hill. Note subvertical rhyolitic dyke. (d, e) Tuff breccias, highly silicified and ferruginized, forming the upper parts of the 108 m hill. Pen is 14 cm long and coin 2.5 cm wide. *f,* Tuff breccia at the summit of the 83 m hill. Coin is 2.5 cm wide. (g) Close-up of tuff breccia forming the Mahadev ni Dhar mound. Part of pen visible is 5 cm long.

rheomorphic deformation, while widespread in the area, is not origin-diagnostic.

Basal autobreccias, and abrupt and steep lava flow fronts fringed by crumble breccias, are common features of rhyolite lavas (e.g. Christiansen & Lipman, 1966; Bonnichsen & Kauffman, 1987; Manley & Fink, 1987; Henry & Wolff, 1992; Ellis *et al.* 2013). They are atypical of lava-like ignimbrites, which are sheet-like and thin gradually away from their vent (Andrews & Branney, 2011). The criterion of steep breccia-fringed fronts only works for young, uneroded lavas, whereas the original geometries of the rheomorphic silicic volcanics of the area and their eruptive vents are both unknown. Crumble breccias characteristically contain an assortment of lava types including vesicular, pumiceous, massive, flow-banded and folded. The dacite at the northern end of the Khalsa Kanthariya Ridge shows an excellent basal autobreccia with vesicular clasts (Fig. 7a–d), and the nearby 71 m hillock is entirely composed of this probable autobreccia as well (Fig. 7e). In fact, possible autobreccias are also exposed on the Hindorna Hill (also 71 m, Fig. 7g) and the nearby 41 m and 51 m hillocks, which are composed of intensely rheomorphic rhyolite (Figs. 5f, i, 7h, i). These hillocks may constitute southwestward extensions of the Rajula Ridge.

Among petrographic criteria, broken crystals are not a diagnostic indicator of pyroclastic origin (Henry & Wolff, 1992; Sheikh *et al.* 2020b). An important criterion, that vitroclasts (glass shards and pumice fragments) must occur in ignimbrites but are absent in lavas, is not always straightforward to apply. This is because the lava-like flow, intense welding and devitrification and recrystallization of extremely high-grade ignimbrites often obscure the original vitroclastic textures, and extremely compacted, stretched and recrystallized vitroclasts can mimic flow bands in rhyolite lavas (e.g. Schmincke & Swanson, 1967; Wolff & Wright, 1981; Smith, 2002; Andrews & Branney, 2011; Ellis *et al.* 2013; Naik *et al.* 2021).

Rather than depending on a single criterion, therefore, we use the above criteria in combination. We note that the confirmed and probable basal autobreccias of the rheomorphic rhyolites and dacites (Fig. 7), their unbroken phenocrysts (Fig. 14) and their microcrystalline, lithoidal groundmasses and lack of vitroclasts or pyroclasts (Fig. 14) all suggest lavas. As argued by Cassidy *et al.* (2018) and Popa *et al.* (2021), silicic magmas have a tendency to erupt effusively rather than explosively when they are crystal-rich (>30 vol.% crystals) and ascend slowly in their conduits and thus degas extensively, both these conditions leading to high viscosities.

https://doi.org/10.1017/S0016756823000432 Published online by Cambridge University Press

Figure 13. (Colour online) Dykes and mafic enclaves found in the study area. (a) Multiple-injection mafic dyke near Adsang. Six identifiable columnar rows are numbered 1 to 6, sample RJ21/22 represents the easternmost columnar row. (b) The Chhapariyali silicic dyke studied by Cucciniello *et al.* (2020) and Sheikh *et al.* (2023). The dyke in the foreground, with a N57° trend, continues as a spine in the hill in the distance, made up of gently dipping basaltic lava flows. (c) N40°-striking rhyolitic dyke intruding basalt at Navagam-Meriyana, person for scale. (d) Subvertical flow banding in the Navagam-Meriyana rhyolitic dyke, person for scale. (e) One of several rhyolitic dykes intruding tuffs in the 108 m hill, Barman Nana Ridge (BNR, see also Fig. 10c). (f) Dolerite dyke in the Devgana tuff breccia ridge. (g) Mafic enclaves of various sizes in the rhyolite dyke SS34 of Cucciniello *et al.* (2020) at Moti Vadal. Vertical face, hammer 33 cm long. (h) Large and small mafic enclaves in rheomorphic rhyolite of the Moti Kherali Ridge (MKR) at Barbtana. Vertical face, pen 14 cm long. (i) Mafic enclaves in the rhyolitic lapilli tuff forming the 83 m hill, Barman Nana Ridge. Coin is 2.5 cm wide.

This may well explain why the rheomorphic rhyolites and dacites of the area, all notably crystal-rich (Fig. 14), erupted as lavas.

Christiansen and Lipman (1966) and Smith and Houston (1994) ascribed asymmetrical isoclinal recumbent folds in rhyolite lavas, found particularly near flow bases, to shearing associated with the lateral movement of lava away from the vent, and the upright folds found particularly in the upper parts of the lavas to lateral shortening during flow. The asymmetrical folds (Figs. 5f, 6g) indicate that simple shear was a significant component of the rheomorphic deformation. The F_1 folds are in fact polyclinal, with varying orientations of their axial planes (Fig. 6g). This may be a consequence of the heterogeneous, unconfined nature of the F_1 folding in an open and unconfined surface environment, or modification of the F_1 folds by F_2 folding with the same characteristics in the same environment. Modification and reorientation of early-formed folds during progressive shear, involving stretching and amplification of pre-existing curvilinear folds, formed the sheath folds (Fig. 6e) (e.g. Reber *et al.* 2013; Bullock *et al.* 2018), whereas ductile necking due to layer-parallel stretching during rheomorphic flow produced boudins (Fig. 6f) (Smith, 2002). The development of F_1 tight-isoclinal folds (Figs. 5h, 6b–d), outcrop-scale sheath folds (Fig. 6e) as well as F_1 tight-isoclinal folds superimposed by F_2 folds producing Type-3 interference patterns (Ramsay, 1967, Fig. 5h, 6b, g), all without the formation of penetrative axial planar cleavage, indicate dynamic and heterogeneous non-coaxial progressive ductile deformation (Flinn, 1962; Ramsay, 1979) during rheomorphic flow of the lava.

Columnar joints in the rheomorphic rhyolites and dacites (Fig. 4f) cross-cut flow bands and folds, and thus formed at a late stage, by cooling and contraction of the lavas after they had stopped moving. The continuous columnar joints from bottom to top indicate the lavas to be single cooling units and require the timescales of emplacement to have been much shorter than the timescales of cooling. The centimetre-thick vertical rhyolitic dykelet with sharp margins cutting the basal autobreccia of the Khalsa Kanthariya dacite (Fig. 7d) is interpreted as an auto-intrusion of left-over melt into a brittle, solid host.

https://doi.org/10.1017/S0016756823000432 Published online by Cambridge University Press

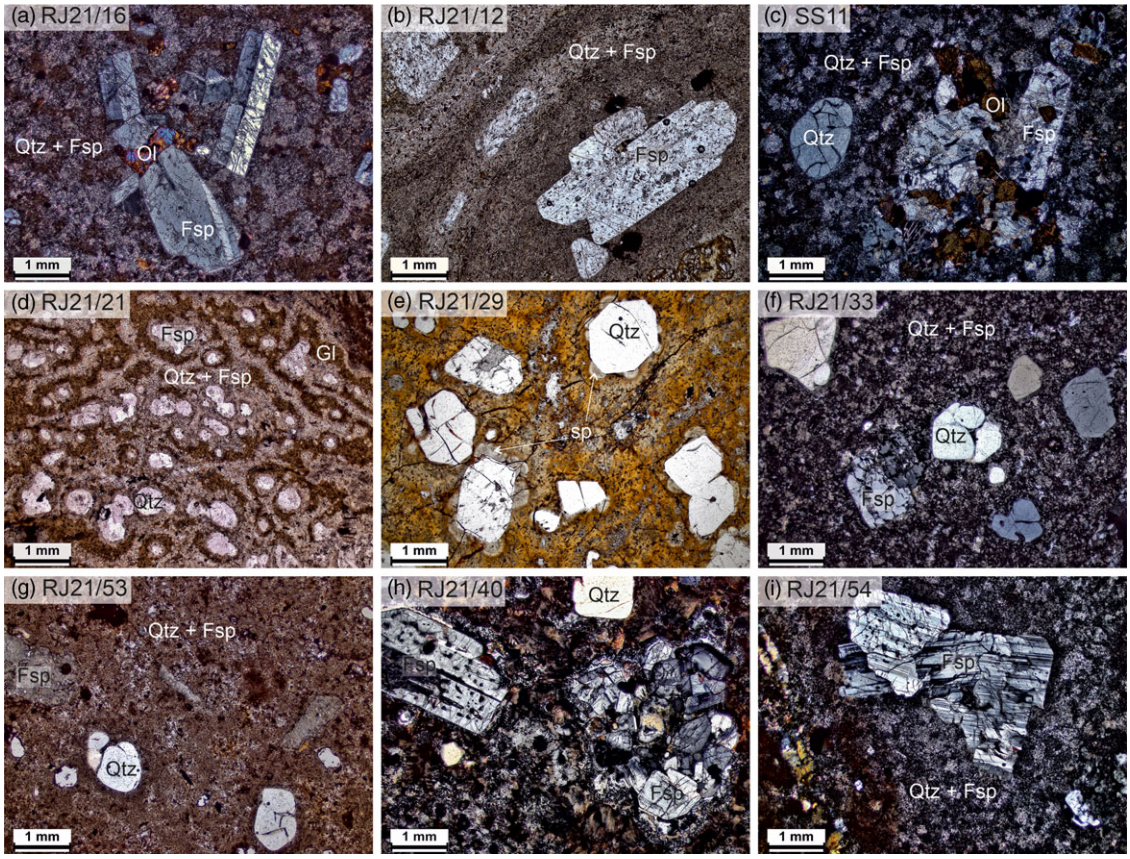

Figure 14. (Colour online) Textural features of the rheomorphic rhyolites and dacites. Abbreviations used are as follows: Qtz, quartz; Fsp, feldspar; Ol, olivine; Gl, glass; sp, spherulites. (a) RJ21/16, dacite of Barman Mota Ridge, in cross-polarized light (xpl). (b) RJ21/12, dacite of Khalsa Kanthariya Ridge, in plane-polarized light (ppl). (c) SS11, rhyolite of Rajula quarry (xpl). (d) RJ21/21, rhyolite near Samadhiyala (ppl). (e) RJ21/29, rhyolite of Moti Kherali Ridge at Barbtana (ppl). (f) RJ21/33, rhyolite of Moti Kherali Ridge at the potential geosite (xpl). (g) RJ21/53, rhyolite of Khakhbai Hill (ppl). (h) RJ21/40, rhyolite 3 km north of Mandal (xpl). (i) RJ21/54, rhyolite of Bhaguda Hill summit (xpl). Note the crystal-rich nature of all rocks and the absence of vitroclasts.

Rhyolitic lavas, while highly viscous, can flow kilometres or tens of kilometres if the erupted volume is large and the lava effectively retains heat due to a thick solidified crust. Bonnichsen (1982) mentions that the Bruneau-Jarbidge eruptive centre in the Snake River Plain contains about a dozen large rhyolite flows, several of which are ~100 m thick with minimum volumes of 10 km^3 each. The largest, Sheep Creek rhyolite is 42 km long, >250 m thick and has a minimum volume of 200 km^3. The rheomorphic rhyolites and dacites of the study area were evidently large-volume lava flows, though the volumes are difficult to estimate due to subsequent tectonic faulting, erosion and infilling of the structurally depressed areas by alluvium. Sheet-like rhyolitic lava flows (termed *flood rhyolites* by Henry & Wolff, 1992) are comparatively uncommon in the world. However, the numerous examples in the study area (Figs. 4–7), and others described from Mount Pavagadh (Sheikh *et al.* 2020b) and the Alech Hills caldera (Sheth *et al.* 2022a), imply that a significant number of flood rhyolite (and dacite) lavas are present in the northern-northwestern Deccan Traps.

4.a.2. Pitchstones and vitrophyres

We noted that the vitrophyres found in the area commonly underlie rheomorphic rhyolite lavas. We also note that vitroclasts are absent in all the glassy rocks as they are in the rhyolitic rocks (Figs. 14, 15), and that individual rhyolite lavas and underlying vitrophyres have essentially the same mineral assemblages and crystal sizes (Figs. 14, 15). Thus, there are striking petrographic similarities between the rhyolite-vitrophyre pairs exposed 3 km north of Mandal (Figs. 14h, 15c), in the Moti Kherali Ridge at Barbtana (Figs. 14e, 16a) and in the Bhaguda Hill (Figs. 14i, 15h). These observations suggest that most vitrophyres are the chilled bases of the overlying rhyolite lavas. Basal glassy bands chilled against a cold substrate are common in rhyolitic lavas, such as those of the Bruneau-Jarbidge eruptive centre in the Snake River Plain (Bonnichsen, 1982); a Deccan analogue has been described at Mount Pavagadh (Sheikh *et al.* 2020b).

The vitrophyre overlying rhyolite near Kundaliyala (Fig. 8f) may represent the chilled *upper* margin of that rhyolite, or the preserved chilled base of a younger rhyolite subsequently eroded. Vitrophyric portions along the southern margin of the Navagam-Meriyana rhyolitic dyke (Fig. 15i) may mark the parts where the rhyolite magma was chilled in contact with cold country rock. Similar situations have been described in silicic dykes at Chhapariyali (Cucciniello *et al.* 2020; Sheikh *et al.* 2023) and Osham Hill (Naik *et al.* 2021).

The common perlitic cracks in the pitchstones and vitrophyres (Fig. 15) attest to their low-temperature, hydration-assisted devitrification (Ross & Smith, 1955). It is possible that the cracks themselves reflect strain due to rapid cooling and provided the pathways for subsequent hydration (Marshall, 1961; Davis & McPhie, 1996).

https://doi.org/10.1017/S0016756823000432 Published online by Cambridge University Press

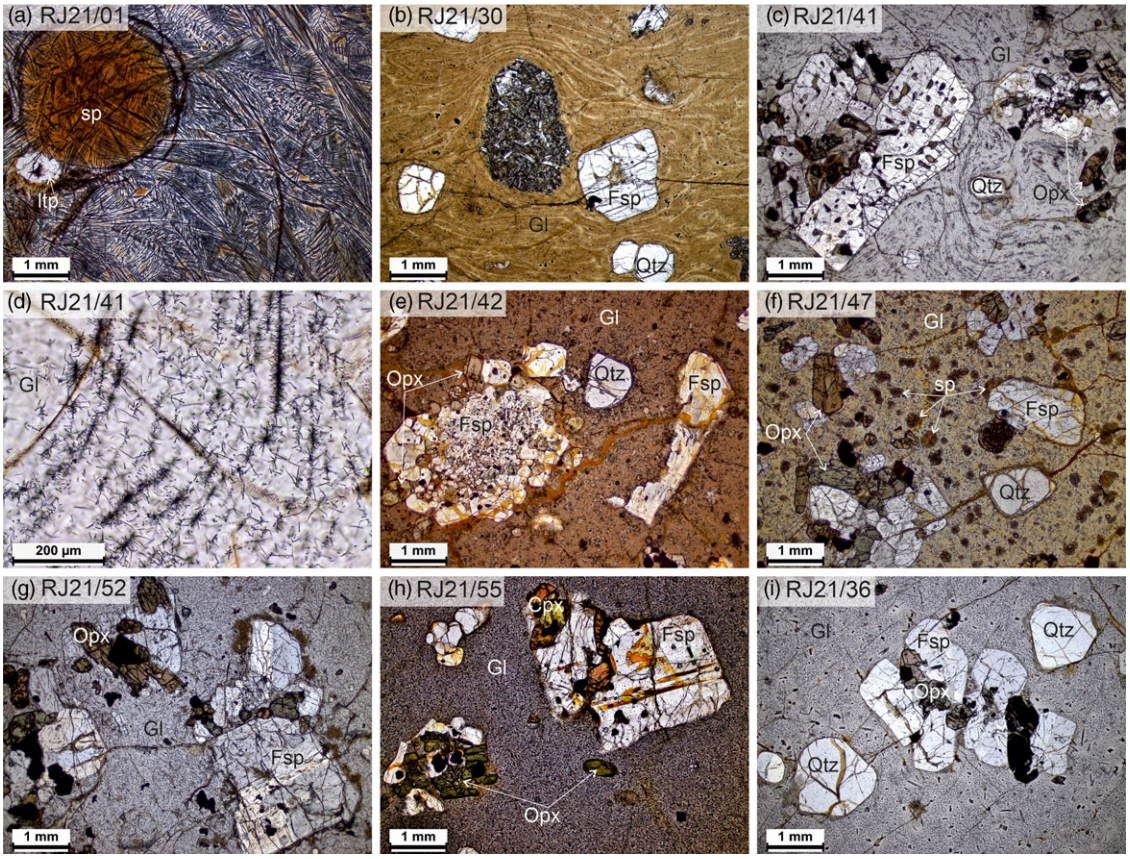

Figure 15. (Colour online) Textural features of the pitchstones and vitrophyres (all photomicrographs in ppl). Abbreviations used are as follows: Qtz, quartz; Fsp, feldspar; Opx, orthopyroxene; Cpx, clinopyroxene; Gl, glass; sp, spherulites; ltp, lithophysae. (a) RJ21/01, fresh pitchstone of Kagvadar. (b) RJ21/30, vitrophyre forming patches within rheomorphic rhyolite in the Moti Kherali Ridge at Barbtana. Note refolded fold around mafic enclave. (c) RJ21/41, vitrophyre 3 km north of Mandal. (d) High-magnification view of RJ21/41 showing trains of innumerable crystallites (many arranged in axiolitic arrangements) that define the flow banding. (e) RJ21/42, vitrophyre of Doliya. (f) RJ21/47, vitrophyre near Zanzarda. (g) RJ21/52, vitrophyre of Khakhbai Hill. (h) RJ21/55, vitrophyre of Bhaguda Hill. (i) RJ21/36, vitrophyre from the southern margin of the Navagam-Meriyana rhyolitic dyke. Note the crystal-rich nature of all rocks and the absence of vitroclasts.

4.a.3. Embayed quartz and crystal cargoes of mafic composition

Quartz phenocrysts in silicic volcanic rocks often show prominent embayments, as seen in several rhyolites and vitrophyres of this study (Figs. 14f, g, 16a). The embayments have been considered by some (e.g. Foster, 1960) as indicating crystal dissolution in surrounding melt. However, these phenocrysts have sharp and smooth boundaries and show no evidence for magmatic corrosion (such as irregular boundaries or trails of melt inclusions). We agree with Vernon (2018) that embayments in quartz may not reflect dissolution (resorption) but rapid cooling, i.e., the embayed quartz grains should be viewed as a kind of skeletal crystals (see also Donaldson & Henderson, 1988).

The large and abundant aggregates of plagioclase and orthopyroxene (with some clinopyroxene and olivine) that are common in the rhyolites and vitrophyres (Figs. 14h, i, 15b, c, e–i) constitute a mafic rock assemblage, namely a norite or an evolved gabbro. They are possible evidence for origin of the silicic magmas by fractional crystallization, i.e., the aggregates are part of the cumulus crystals fractionated from parental mafic melts and were brought up as a crystal cargo by the residual rhyolitic melts. Bending of plagioclase twin lamellae (Fig. 14i) and breakage of individual crystals (Fig. 15e) are features consistent with forceful uprise of the residual rhyolitic melts, arguably aided by volatile enrichment. Broadly similar crystal aggregates have been described in ignimbrites of the Snake River Plain (Ellis *et al.* 2014) and in the Mount Pavagadh rhyolite lava (Sheikh *et al.* 2020b). Szymanowski *et al.* (2015) find evidence for intermediate to mafic (dioritic-gabbroic) mushes stored in mid-crustal reservoirs under the Yellowstone-Snake River Plain province, including a geophysically imaged, 10 km thick, high-density body. We note that the area of the present study is situated over one of several large, circular to ellipsoidal, high gravity anomalies mapped over the Saurashtra region (Chandrasekhar *et al.* 2002).

4.b. Explosive silicic volcanism

4.b.1. Tuffs and ignimbrites

The crystal-vitric tuff of the Moti Kherali Ridge at Barbtana (Fig. 16d, e) is composed dominantly of glass shards, pumice clasts and quartz crystals, with a few alkali feldspar crystals. The cuspate and Y-shaped glass shards represent broken melt films originally separating adjacent gas bubbles and indicate magmatic volatile-driven explosive fragmentation of rising magma experiencing decompression (e.g. Heiken, 1974; Klug & Cashman, 1996; Mader, 1998). In its petrographic features, this tuff closely resembles the nonwelded, crystal-bearing, glass- and pumice-rich ash beds of Mount Pavagadh 260 km to the northeast, with the difference that the dominant crystals in the Barbtana tuff are quartz (Fig. 16d, e) but in the Pavagadh ash beds they are alkali feldspar (Sheikh *et al.*

https://doi.org/10.1017/S0016756823000432 Published online by Cambridge University Press

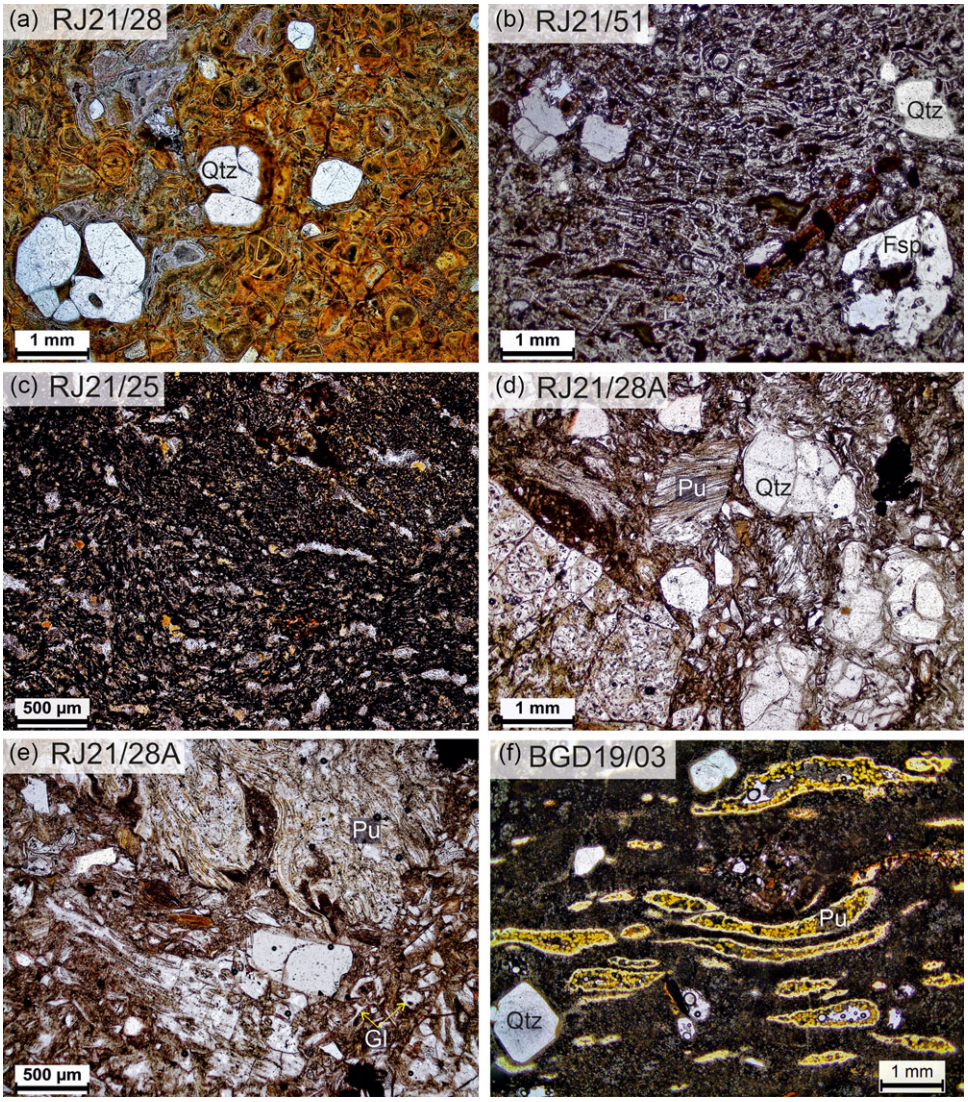

Figure 16. (Colour online) Textural features of two altered vitrophyres, and tuffs and ignimbrites. All photomicrographs are in ppl. Abbreviations used are as follows: Gl, glass or glass shards; Pu, pumice clasts; Qz, quartz; Fsp, feldspar. (a) False vitroclastic texture in RJ21/51, green altered vitrophyre at Khakhbai Hill. (b) False vitroclastic texture in RJ21/28, green-grey altered vitrophyre in the Moti Kherali Ridge at Barbtana. (c) RJ21/25, very fine-grained rhyolite underlying lithophysae-bearing rheomorphic rhyolite at Ghanshyamnagar. (d,e) RJ21/28A, crystal-rich and vitric-rich (pumice-rich) lapilli tuff from Moti Kherali Ridge at Barbtana. (f) Eutaxitic ignimbrite underlying vitrophyre at Bhaguda Hill. Note the innumerable tiny spherulites formed by devitrification of the pumice fiamme. Small transparent circular objects are air bubbles introduced during thin section preparation.

2020b). The Pavagadh ash beds were interpreted by Sheikh *et al.* (2020b) as a thick fallout ash succession derived from many distal Plinian eruptions, possibly in Saurashtra. We similarly interpret the Barbtana tuff (Fig. 16d, e) as a nonwelded crystal-vitric tuff, representing Plinian fallout ash, from a yet unknown vent. Testing for any potential correlations between this tuff and the Pavagadh ash beds with geochronological and geochemical data would be interesting future work.

The extraordinary development of lithophysae in the Longdi-Bhaguda green tuff (Fig. 9g–i) suggests that the magma was exceptionally volatile-rich, and a substantial amount of volatiles was retained in the ash on deposition, causing widespread alteration of the tuff. This requires very rapid deposition which, along with the lack of bedding, suggests deposition from turbulent pyroclastic density currents. Both features are inconsistent with a fallout origin.

The eutaxitic ignimbrites overlying tuffs in the Moti Kherali Ridge at Barbtana (Fig. 8g) and at Bhaguda Hill (Fig. 8h, i) are the products of moderate degrees of welding of vitroclasts. They represent deposition from relatively hot pyroclastic density currents (e.g. Ross & Smith, 1961; Bull & McPhie, 2007). The pumice fragments in them became highly compacted vertically and stretched horizontally (Fig. 16f) due to loading (and additional heating) by younger units: a rheomorphic rhyolite lava, with a chilled basal vitrophyre, is found above the eutaxitic ignimbrite in each case.

Early and recent observations (e.g. Wakhaloo, 1967; Chatterjee, 1969; Krishnamacharlu, 1974; Sheikh *et al.* 2020a, b; Naik *et al.* 2021; Sheth *et al.* 2022a) and those made in the present study together imply that a range of ignimbrite types is present, along with numerous flood rhyolite and dacite lavas, in the northern and northwestern Deccan Traps. As discussed in detail in these recent studies, many striking similarities exist between the effusive-explosive northern-northwestern Deccan silicic volcanism and the much younger (ca. 13–8 Ma) silicic volcanism in the Snake River Plain (e.g. Bonnichsen, 1982; Andrews & Branney, 2011; Ellis *et al.* 2013).

4.b.2. Tuff breccias

Tuff breccias found in the southwestern part of the area form the 4 km long, E-W-trending Barman Nana Ridge and the largely alluvium-covered, E-W-trending Mahadev ni Dhar mound

https://doi.org/10.1017/S0016756823000432 Published online by Cambridge University Press

(Figs. 3, 12a). Both these ridges are interpreted here as pyroclastic eruptive fissures apparently in an *en echelon* configuration (Fig. 3). The northwestern tuff breccia ridges, namely the Sakhpur and Bovadi ridges (Fig. 2), are also interpreted here as huge *en echelon* pyroclastic eruptive fissures with minimum original lengths of 14 km and 22 km, respectively. These ridges cannot simply be erosional remnants of an originally widespread tuff breccia blanket: not only are they linear, but exposed contacts of the Sakhpur Ridge with the host basaltic lava flows at Nana Rajkot are subvertical, confirming that the ridges represent linear vents or vent alignments.

Sethna *et al.* (2001) have suggested that ridges of silicic breccia in this area (some likely the ones described here) are fault-bounded ridges, as indicated by slickensides and silicification. We consider these ridges as primary eruptive fissures, now standing in relief over the basalts and alluvium, owing to the greater erosional resistance of the rhyolitic (and extensively silicified) tuff breccias. Any slickensides observed we consider to be secondary and small-scale features. The extensive secondary silicification (and ferruginization) observed throughout these ridges (Figs. 10–12) is as expected, noting that when fluid-rich, silicic magmas are more likely to erupt explosively than effusively (e.g. Cassidy *et al.* 2018; Popa *et al.* 2021).

At Talaja Hill (Fig. 11a–f), the stratigraphic and structural relationships of the pumice with the tuff breccias are not clear, and the volcanological features are exceedingly complex. We broadly view the hill as a Plinian eruptive fissure (possibly a central-type vent) with an exposed core of pumice blocks, overlain by tuff breccias.

The N-S-trending Devgana Ridge (Fig.11g, h) lies near the ENE-WSW-trending Eastern Saurashtra mafic dyke swarm and was considered by Sheth *et al.* (2013) to be an altered silicic dyke in the swarm. We interpret this ridge as a pyroclastic eruptive fissure comparable to the others described, and a part of the Shihor-Rajpara and Chogat-Chamardi rhyolite-granophyre cluster nearby (Misra, 1999; Chatterjee & Bhattacharji, 2001, 2004; Sheth *et al.* 2011, Fig. 1).

4.c. Spherulites and lithophysae

As noted, spherulites form due to heterogeneous nucleation in highly supercooled silicic melts or by devitrification of glass. Good evidence for the former mechanism is provided by the many spherulites in the rheomorphic rhyolite of Moti Kherali Ridge, which have nucleated on corners of quartz crystals (Fig. 14e). Spherulites are also present in the groundmass between crystals, however. The spherulites, which are prolific in the altered bands of pitchstone at Kagvadar (Fig. 8a, c, d), may be products of devitrification. As regards the coarse banding of this pitchstone with fresh and spherulitic bands, Kshirsagar *et al.* (2012) noted that spherulites may nucleate preferentially along certain zones in a rock body as dictated by the thermal profile (Manley & Fink, 1987), depth and cooling rate or even post-eruption, structure-controlled hydration (Davis & McPhie, 1996). The fact that spherulites grew across the textural elements of the Kagvadar pitchstone without displacing them (Fig. 15a) suggests that they grew (or continued to grow) at a late stage below the glass transition temperature (Vernon, 2018).

The extraordinary development of lithophysae in the Longdi-Bhaguda green tuff (Fig. 9g–i) was first described by Misra (1976, 1981, 1999); he correctly noted that these objects lacking a radial internal structure were not spherulites. He interpreted them as 'rhyolitic lava bombs' produced by pyroclastic activity, and the twins-triplets-quadruplets as 'fused lava bombs', and cited Bhaguda-Longdi as the best locality to study explosive volcanism in the Deccan Traps. Kshirsagar *et al.* (2012) recognized these features as thundereggs (i.e. lithophysae filled with secondary minerals) because of the absence of a radial fibrous structure observed in hand specimen (corroborated by their thin section observations), and secondary silica fills in their central cavities and fractures. The twins, triplets and quadruplets were interpreted as lithophysae which started growing on nearby nuclei and coalesced upon enlargement. In contrast to Misra (1976, 1981, 1999), Kshirsagar *et al.* (2012) interpreted the host rocks of the lithophysae as subvolcanic intrusions. Subsequent and better field observations (Sheikh *et al.* 2020a and this study) leave no doubt that the host rocks of the lithophysae are volcanic and pyroclastic, namely the eutaxitic ignimbrite (Fig. 8h, i) and the pale green tuff (Fig. 9g, h). These observations corroborate Misra (1976, 1981, 1999), except for the misidentification of volcanic bombs, and we consider that the area is indeed *one of the* best localities to study pyroclastic volcanism in the Deccan Traps (see Sheikh *et al.* 2020a, b; Naik *et al.* 2021; Sheth *et al.* 2022a).

4.d. Mafic enclaves

Mafic enclaves are common in silicic dykes in the area (Fig. 13g, see also Cucciniello *et al.* 2020; Sheikh *et al.* 2023). These indicate the phenomenon of composite intrusion and magma mingling, expected to occur when a relatively hot mafic magma gets injected into cooler but rheologically essentially liquid silicic magma in a chamber or conduit (e.g. Yoder, 1973; Snyder, 2000). The resultant gravitational and fluid dynamical instabilities break up the mafic magma into blobs and clots. The two magmas do not mix owing to their temperature, composition and rheology contrasts, and mafic enclaves are left within the silicic host as heat is finally lost from the system. If eruption occurs before this, a volcanic unit containing the mingled enclaves forms, for example, the Moti Kherali Ridge rheomorphic rhyolite at Barbtana (Fig. 13h). In fact, mafic magma recharge may itself have been responsible for the silicic magma being expelled from its chamber and even erupting (e.g. Snyder, 2000). Progressively advanced disruption of the intruding mafic magmas injected within rhyolitic magmas is evident from the outcrop-scale (Fig. 13h) to microscopic-scale (Fig. 15b) enclaves observed within the Moti Kherali Ridge rheomorphic rhyolite and the vitrophyre patches in it.

The widespread occurrences of mafic enclaves in the area show that mafic and silicic magmatism overlapped both in time and in space. The crystal cargoes of mafic composition common in the rhyolites and vitrophyres of the area (Figs. 14h, i, 15b, c, e–i) are comparable to those in the Mount Pavagadh rhyolite lava and the Chhapariyali rhyolite dyke; they were similarly derived from disaggregation of gabbroic cumulate mushes in magma chambers (see Sheikh *et al.* 2020b, 2023).

4.e. Potential environmental impact and geochronological aspects

The rheomorphic rhyolites and dacites (Figs. 2–4) are mere remnants of what were evidently large-volume flood lavas. Similarly, the silicic tuff breccia ridges represent large-scale explosive volcanism: the combined Sakhpur and Bovadi ridges (Fig. 2) constitute a huge *en echelon* pyroclastic eruptive fissure at least 35 km long, and probably extending further both to the north and south under the Quaternary alluvium. The massive effusive

https://doi.org/10.1017/S0016756823000432 Published online by Cambridge University Press

and explosive silicic eruptions in the study area are thus important not only for understanding the physical volcanology of the Deccan Traps and CFB provinces but also for their probable environmental impact.

Sheikh *et al.* (2020a, b) suggested that the northern-northwestern Deccan silicic volcanism, both effusive and explosive, may have played a significant role in the K/Pg boundary mass extinction, and a single CA-ID-TIMS $^{206}Pb/^{238}U$ date of 65.765 ± 0.018 Ma (2σ, Basu *et al.* 2020) available for the granophyre ring dyke of the Alech Hills caldera supports this possibility. Geochronological work on the silicic rocks of the present study area is scarce and with limited interpretative value. Chatterjee & Bhattacharji (2001) provided K-Ar ages on mafic and silicic dykes around Rajula that range from 72.6 ± 2.2 Ma to 63.0 ± 1.0 Ma (2σ errors). Basu *et al.* (2020) dated a rock sample (R7 in their map in Fig. S5C) and provided a maximum emplacement age of 65.784 ± 0.031 Ma (2σ) (CA-ID-TIMS $^{206}Pb/^{238}U$ date on the youngest zircon). It is unclear what geological unit and rock type this sample represents. The distances shown in their map, with an incorrect scale bar, are five to six times the actual distances, and the Chogat-Chamardi complex does not exist at the location shown. There is thus a great scope and need for extensive geochronological and geochemical work on the mafic and particularly the silicic rock units of the area, which must, however, be based on accurate geological maps constructed from ground truth.

4.f. Volcanotectonic aspects

The map pattern of the numerous cuestas of rheomorphic rhyolites and dacites (Fig. 3), and the basaltic cuestas which mimic them, reveals a gradual and systematic shift in their structural trends. The volcanic units in the southwestern part of the area strike NNE-SSW, those in the broad central part strike NE-SW and those in the northeastern part strike ENE-WSW. Considered together the strike ridges define a gentle arc, convex to the north, in which all volcanic units consistently dip towards the east-southeast (at ~15°). Kshirsagar *et al.* (2012) suggested that the silicic units were cone sheets fed by a plutonic centre. This centre is believed to be now submerged beneath the Arabian Sea, an area known to have experienced major post-Deccan downfaulting and subsidence (e.g. Yatheesh, 2020). We note that the silicic units are too thick to be cone sheets, and they conformably overlie basaltic lava flows in exposed stratigraphic sections of the ridges. They also have all the features of eruptive units including rheomorphic deformation and, notably, basal autobreccias. These volcanic units are excellent examples of flood rhyolite and dacite lavas, and detailed structural mapping of their rheomorphic deformation features as a guide to their emplacement dynamics should be exciting future work.

The structural-homoclinal ridges of dipping basaltic and silicic volcanics (Figs. 2, 3) were correctly identified as such by Misra (1976, 1981, 1999). Because of their linearity and great lengths, these ridges have often been erroneously interpreted as dykes, both in early work (e.g. Auden, 1949) and in recent work (Mittal *et al.* 2021). There are indeed many ridges formed by dykes, and those formed by the silicic tuff breccias (Figs. 2, 3). The structural ridges of the basalts, rhyolites and dacites which consistently dip southeast provide evidence for extensive block-faulting at this classical rifted volcanic margin. Direct evidence for faulting is not easy to find, however, because of the extensive erosion and infilling of the structurally depressed areas by alluvium.

The uniformly seaward-dipping, structurally disturbed, basaltic and silicic Deccan volcanic sequence in the area (Figs. 2, 3) constitutes a regional-scale coastal flexure zone, here termed the Southeastern Saurashtra flexure. This is comparable to the Panvel flexure of the western Deccan Traps and flexures in other CFB provinces located on rifted continental margins (e.g. Dessai & Bertrand, 1995; Klausen & Larsen, 2002; Klausen, 2009). The Southeastern Saurashtra flexure zone is large: cuestas with seaward dip slopes are found everywhere from Barman Mota to Jesar to the northeast, and eastwards up to Talaja, a strike distance of 80 km (Figs. 1, 2). The flexure zone extends west and southwest of our study area in Fig. 2 into the Gir forest and Asiatic lion sanctuary (Fig. 1), where geological studies are necessarily limited and quite dated (Chatterjee, 1932; Auden, 1949; Krishnaswamy, 1966).

5. Conclusions

Silicic magmatism, though minor overall in the ~65.5 Ma Deccan Traps CFB province of India, was widespread and voluminous in the Saurashtra peninsula in the northwest. The area of the present study, around the towns of Rajula-Savarkundla-Gariyadhar-Talaja in southeastern Saurashtra, provides excellent insights into the varied styles of silicic volcanism following the flood basalt eruptions. Large-scale effusive silicic eruptions are represented in crystal-rich, strongly rheomorphic rhyolite and dacite lava flows, often with chilled basal vitrophyres. Large-scale explosive eruptions are represented in tuffs and ignimbrites, deposited by ash falls and pyroclastic density currents, and in voluminous tuff breccias, representing pyroclastic eruptive fissures. Spherulites and lithophysae are found in several of the volcanic rocks, and the Bhaguda-Longdi green tuff, in particular, contains extraordinary numbers (tens of thousands) of lithophysae, suggesting an exceptionally volatile-rich silicic magma.

Our results highlight the value of combined field data and textural information obtained with the microscope as a powerful tool in solving volcanological problems. They also highlight the many physical similarities between silicic volcanism (both explosive and effusive) in the northern-northwestern Deccan Traps and in the Snake River Plain, discussed in detail by Sheikh *et al.* (2020a, b), Naik *et al.* (2021) and Sheth *et al.* (2022a). Mafic and silicic dykes are also common in the area, and mingled mafic enclaves found within several silicic dykes and some volcanic units suggest that mafic and silicic magmas often overlapped both in time and space. The numerous structurally controlled homoclinal ridges of rheomorphic silicic lavas and underlying basalts, with dip slopes towards the Arabian Sea, provide evidence for extensive block faulting at this classical volcanic rifted margin.

Supplementary material. The supplementary material for this article can be found at [https://doi.org/10.1017/S0016756823000432].

Acknowledgements. Fieldwork was supported by an Institution of Eminence (IoE) research grant (No. Dev. Scheme 6031, PFMS Scheme 3254) from the BHU to Alok Kumar (Principal Investigator, Collaborator: H. Sheth). A. Naik was supported by a PhD Research Fellowship of the Council of Scientific and Industrial Research (CSIR), Government of India (File No. 09/087(0908)/2017-EMR-I) and an IIT Bombay Institute Post-Doctoral Fellowship (File No. HR-1 (HRM-1)/Rect/33/2022/20003002). J. M. Sheikh was supported by a Malaviya Postdoctoral Fellowship of the BHU (IoE Scheme, Ref. No.: IoE/MPDF/2020-21/14). We thank K. S. Misra for interesting discussions on Saurashtra field geology, and N. Prabhakar and N. Sequeira for discussing some of the rheomorphic deformation features. Much of the study area, while outside the official Gir forest and Asiatic lion sanctuary, is the home of that magnificent and

noble animal. We thank the natives of its many villages, friendly and welcoming both to humans and lions, for their guidance, kindness and incomparable hospitality.

The manuscript was considerably improved by journal reviews from Ciro Cucciniello and an anonymous reviewer, and the editorial work of Eleanor Jennings and Tim Johnson.

References

Allen RL (1988) False pyroclastic textures in altered silicic lavas, with implications for volcanic-associated mineralisation. *Economic Geology* **83**, 424–1446.

Anderson Jr JE (1969) Development of snowflake texture in a welded tuff, Davis Mountains, Texas. *Geological Society of America Bulletin* **80**, 2075–80.

Andrews GDM and Branney MJ (2011) Emplacement and rheomorphic deformation of a large, lava-like rhyolitic ignimbrite: Grey's Landing, southern Idaho. *Geological Society of America Bulletin* **123**, 725–43.

Auden JB (1949) Dykes in western India – a discussion of their relationships with the Deccan Traps. *Transactions of National Institute of Sciences of India* **3**, 123–57.

Ayalew D, Barbey P, Marty B, Reisberg L, Yirgu G and Pik R (2002) Source, genesis, and timing of giant ignimbrite deposits associated with Ethiopian continental flood basalts. *Geochimica et Cosmochimica Acta* **66**, 1429–48.

Baksi AK (2014) The Deccan Trap – Cretaceous-Palaeogene boundary connection; new $^{40}Ar/^{39}Ar$ ages and critical assessment of existing argon data pertinent to this hypothesis. *Journal of Asian Earth Sciences* **84**, 9–23.

Bandopadhyaya S (1976) Acid ring dykes and lava flows in Deccan Trap basalt, Alech Hills, Saurashtra, Gujarat. In *Proceedings of Symposium on Deccan Trap & Bauxite* (eds B Prasad and BS Manjrekar), pp. 158–63. Kolkata: Geological Survey of India Special Publication 14.

Banerjee AC (1998) Report on petrochemical characters of volcanic-subvolcanic acid rocks of Rajula area, Amreli District of Gujarat (Progress Report for the Field Season 1993–94). *Geological Survey of India*, 54 p.

Banerjee AC, Raj D and Roychowdhury M (2000) Gold and PGM contents in a subvolcanic Deccan picrite of Saurashtra, Gujarat. *Journal of Geological Society of India* **56**, 625–32.

Basu AR, Chakrabarty P, Szymanowski D, Ibanez-Mejia M, Schoene, B, Ghosh N and Georg RB (2020) Widespread silicic and alkaline magmatism synchronous with the Deccan flood basalts, India. *Earth and Planetary Science Letters* **552**, art. 116616. doi: 10.1016/j.epsl.2020.116616.

Benson GT and Kittleman LR (1968) Geometry of flow layering in silicic lavas. *American Journal of Science* **266**, 277–98.

Bonnichsen B (1982) Rhyolite lava flows in the Bruneau-Jarbidge eruptive centre, southwestern Idaho. In *Cenozoic Geology of Idaho* (eds B Bonnichsen and RM Breckenridge), pp. 283–320. Boise, Idaho: Idaho Bureau of Mines and Geology Bulletin 26.

Bonnichsen B and Kauffman DF (1987) Physical features of rhyolite lava flows in the Snake River Plain volcanic province, southwestern Idaho. In *The Emplacement of Silicic Domes and Lava Flows* (ed JH Fink), pp. 119–45. Boulder: Geological Society of America Special Paper 212.

Breitkreuz C (2013) Spherulites and lithophysae – 200 years of investigation on high-temperature crystallisation domains in silica-rich volcanic rocks. *Bulletin of Volcanology* **75**, art. 705. doi: 10.1007/s00445-013-0705-6.

Bryan SE, Riley TR, Jerram DA, Stephens CJ and Leat PT (2002) Silicic volcanism: an undervalued component of large igneous provinces and volcanic rifted margins. In *Volcanic Rifted Margins* (eds MA Menzies, SL Klemperer, CJ Ebinger & J Baker), pp. 99–120. Boulder: Geological Society of America Special Paper 362.

Bryan SE, Ukstins Peate I, Peate DW, Self S, Jerram DA, Mawby MR, Marsh JS and Miller JA (2010) The largest volcanic eruptions on earth. *Earth-Science Reviews* **102**, 207–29.

Bull KF and McPhie JM (2007) Fiamme textures in volcanic successions: flaming issues of definition and interpretation. *Journal of Volcanology and Geothermal Research* **164**, 205–16.

Bullock LA, Gertisser R and O'Driscoll B (2018) Emplacement of the Rocche Rosse rhyolite lava flow (Lipari, Aeolian Islands). *Bulletin of Volcanology* **80**, art. 48. doi: 10.1007/s00445-018-1222-4.

Cassidy M, Manga M, Cashman K and Bachmann B (2018) Controls on explosive-effusive volcanic eruption styles. *Nature Communications* **9**, art. 2839. doi: 10.1038/s41467-018-05293-3.

Chandrasekhar DV, Mishra DC, Poornachandra Rao GVS and Mallikharjuna Rao J (2002) Gravity and magnetic signatures of volcanic plugs related to Deccan volcanism in Saurashtra, India and their physical and chemical properties. *Earth and Planetary Science Letters* **201**, 277–92.

Chatterjee N and Bhattacharji S (2001) Origin of the felsic and basaltic dykes and flows in the Rajula-Palitana-Sihor area of the Deccan Traps, Saurashtra, India: a geochemical and geochronological study. *International Geology Review* **43**, 1094–116.

Chatterjee N and Bhattacharji S (2004) A preliminary geochemical study of zircons and monazites from Deccan felsic dykes, Rajula, Gujarat, India: implications for crustal melting. In *Magmatism in India through Time* (eds HC Sheth & K Pande), pp. 533–42. Bengaluru: Proceedings of the Indian Academy of Sciences (Earth & Planetary Sciences) 113.

Chatterjee SC (1969) On the rhyolites of Pavagad Hill. *Current Science* **38**, 293–4.

Chatterjee SK (1932) Petrology of the igneous rocks from the west Gir forest, Kathiawar, India. *Journal of Geology* **40**, 154–63.

Chaurasia PK and Jain LS (2002) *District Resource Map Bhavnagar District, Gujarat*. Kolkata: Geological Survey of India.

Christiansen RL and Lipman PW (1966) Emplacement and thermal history of a rhyolite flow near Fortymile Canyon, southern Nevada. *Geological Survey of America Bulletin* **77**, 671–84.

Cross W (1891) Constitution and origin of spherulites in acid eruptive rocks. *Philosophical Society of Washington Bulletin* **11**, 411–49.

Cucciniello C, Avanzinelli R, Sheth H and Casalini M (2022) Mantle and crustal contributions to the Mount Girnar alkaline plutonic complex and the circum-Girnar tholeiitic-silicic intrusions of Saurashtra, northwestern Deccan Traps. *Journal of Petrology* **63**, art. gac007. doi: 10.1093/petrology/egac007.

Cucciniello C, Choudhary AK, Pande K and Sheth H (2019) Mineralogy, geochemistry and ^{40}Ar-^{39}Ar geochronology of the Barda and Alech complexes, Saurashtra, northwestern Deccan Traps: early silicic magmas derived by flood basalt fractionation. *Geological Magazine* **156**, 1668–90.

Cucciniello C, Sheth H, Duraiswami RA, Wegner W, Koeberl C, Das T and Ghule V (2020) The Southeastern Saurashtra dyke swarm, Deccan Traps: magmatic evolution of a tholeiitic basalt–basaltic andesite–andesite–rhyolite suite. *Lithos* **376–377**, art. 105759. doi: 10.1016/j.lithos.2020.105759.

Davis B and McPhie J (1996) Spherulites, quench fractures and relict perlite in a Late Devonian rhyolite dyke, Queensland, Australia. *Journal of Volcanology and Geothermal Research* **71**, 1–11.

Dessai AG and Bertrand H (1995) The 'Panvel Flexure' along the western Indian continental margin: an extensional fault structure related to Deccan magmatism. *Tectonophysics* **241**, 165–78.

Donaldson CH and Henderson CMB (1988) A new interpretation of round embayments in quartz crystals. *Mineralogical Magazine* **52**, 27–33.

Ellis BS, Bachmann O and Wolff JA (2014) Cumulate fragments in silicic ignimbrites: the case of the Snake River Plain. *Geology* **42**, 431–4.

Ellis BS, Wolff JA, Boroughs S, Mark DF, Starkel WA and Bonnichsen B (2013) Rhyolitic volcanism of the central Snake River Plain: a review. *Bulletin of Volcanology* **75**, art. 745. doi: 10.1007/s00445-013-0745-y.

Fedden F (1884) The geology of the Kathiawar peninsula in Gujarat. *Geological Survey of India Memoir* **21**, 73–136.

Flinn D (1962) On folding during three-dimensional progressive deformation. *Quaternary Journal of the Geological Society* **118**, 385–433.

Foster RJ (1960) Origin of embayed quartz crystals in volcanic rocks. *American Mineralogist* **45**, 892–4.

Halder M, Paul D and Sensarma S (2021) Rhyolites in continental mafic large igneous provinces: petrology, geochemistry and petrogenesis. *Geoscience Frontiers* **12**, 53–80.

Halder M, Paul D and Stracke A (2023) Petrogenesis of the Girnar complex in the Deccan Traps province, India. *Journal of Petrology* **64**, art. egad013. doi: 10.1093/petrology/egad013.

Hatch FH, Wells AK and Wells MK (1983) *Petrology of the Igneous Rocks*, 13th edn. London: Thomas Murby, 551 p.

Heiken G (1974) Atlas of Volcanic Ash. *Smithsonian Contributions in Earth Sciences*, 101 p. doi: 10.5479/si.00810274.12.1.

Henry CD and Wolff JA (1992) Distinguishing strongly rheomorphic tuffs from extensive silicic lavas. *Bulletin of Volcanology* **54**, 171–86.

Iddings JP (1892) On the crystallisation of igneous rocks. *Philosophical Society of Washington Bulletin* **11**, 71–112.

Klausen MB (2009) The Lebombo monocline and associated feeder dyke swarm: diagnostic of a successful and highly volcanic rifted margin? *Tectonophysics* **468**, 42–62.

Klausen MB and Larsen HC (2002) East Greenland coast-parallel dyke swarm and its role in continental breakup. In *Volcanic Rifted Margins* (eds MA Menzies, SL Klemperer, CJ Ebinger & J Baker), pp. 137–62. Boulder: Geological Society of America Special Paper 362.

Klug C and Cashman KV (1996) Permeability development in vesiculating magmas: implications for fragmentation. *Bulletin of Volcanology* **58**, 87–100.

Krishnamacharlu T (1974) Ignimbrite flows from Rajula, Saurashtra, India. *Geological Magazine* **111**, 49–54.

Krishnaswamy S (1966) Geology of a part of the eastern Gir Forest (Kathiawar). *Records of Geological Survey of India* **94**, 211–20.

Kshirsagar PV, Sheth HC, Seaman SJ, Shaikh B, Mohite P, Gurav T and Chandrasekharam D (2012) Spherulites and thundereggs from pitchstones of the Deccan Traps: geology, petrochemistry, and emplacement environments. *Bulletin of Volcanology* **74**, 559–77.

Lofgren G (1971) Spherulitic textures in glassy and crystalline rocks. *Journal of Geophysical Research* **76**, 5635–48.

Luchetti ACF, Nardy AJR and Madeira J (2018) Silicic, high- to extremely high-grade ignimbrites and associated deposits from the Paraná Magmatic Province, southern Brazil. *Journal of Volcanology and Geothermal Research* **355**, 270–86.

Mader H (1998) Conduit flow and fragmentation. In *The Physics of Explosive Volcanic Eruptions* (eds JS Gibert & RSJ Sparks), pp. 51–71. London: Geological Society Special Publication 145.

Manley CR and Fink JH (1987) Internal textures of rhyolite flows as revealed by research drilling. *Geology* **15**, 549–52.

Marshall RR (1961) Devitrification of natural glass. *Geological Society of America Bulletin* **72**, 1493–520.

Mathur KK, Dubey VS and Sharma NL (1926) Magmatic differentiation in Mount Girnar. *Journal of Geology* **34**, 289–307.

McPhie J, Doyle M and Allen R (1993) *Volcanic Textures: A Guide to the Interpretation of Textures in Volcanic Rocks*. Hobart: CODES: University of Tasmania, 196 p.

Misra KS (1976) A preliminary note on the Deccan Trap basaltic flows in the vicinity of Rajula in Saurashtra. In *Proceedings of Symposium on Deccan Trap & Bauxite* (eds B Prasad & BS Manjrekar), pp. 18–9. Kolkata: Geological Survey of India Special Paper 14.

Misra KS (1981) The tectonic setting of Deccan volcanics in southern Saurashtra and southern Gujarat. In *Deccan Volcanism* (eds KV Subbarao and RN Sukheswala), pp. 81–6. Bengaluru: Geological Society of India Memoir 3.

Misra KS (1999) Deccan volcanics in Saurashtra and Kutch, Gujarat, India. In *Deccan Volcanic Province* (ed KV Subbarao), **43**, pp. 325–34. Bengaluru: Geological Society of India Memoir.

Mittal T, Richards MA and Fendley IM (2021) The magmatic architecture of continental flood basalts I: observations from the Deccan Traps. *Journal of Geophysical Research: Solid Earth* **126**, art. e2021JB021808. doi: 10.1029/2021JB021808.

Naik A, Sheth H, Sheikh JM and Kumar A (2021) Extremely high-grade, lava-like rhyolitic ignimbrites at Osham Hill, Saurashtra, northwestern Deccan Traps: stratigraphy, structures, textures, and physical volcanology. *Journal of Volcanology and Geothermal Research* **419**, art. 107389. doi: 10.1016/j.jvolgeores.2021.107389.

Polo LA, Janasi VA, Giordano D, Lima EF, Cañon-Tapia E and Roverato M (2018) Effusive silicic volcanism in the Paraná magmatic province, south Brazil: evidence for locally-fed lava flows and domes from detailed field work. *Journal of Volcanology and Geothermal Research* **355**, 204–18.

Popa R-G, Bachmann O and Huber C (2021) Explosive or effusive style of volcanic eruption determined by magma storage conditions. *Nature Geosciences* **14**, 781–6.

Raj D and Jain LS (2002) *District Resource Map Amreli District, Gujarat*. Kolkata: Geological Survey of India.

Ramasamy SM (1995) Deformation tectonics of Deccan volcanics of southern Saurashtra, India and its relation to western extension of Narmada lineament. In *Magmatism in Diverse Tectonic Settings* (eds RK Srivastava & U Chandra), pp. 195–208. New Delhi: Oxford & IBH Publishers.

Ramsay DM (1979) Analysis of rotation of folds during progressive deformation. *Geological Society of America Bulletin* **98**, 732–8.

Ramsay JG (1967) *Folding and Fracturing of Rocks*. New York: McGraw-Hill, 568 p.

Reber JE, Dabrowski M, Galland O and Schmid DW (2013) Sheath fold morphology in simple shear. *Journal of Structural Geology* **53**, 15–26.

Rooney TO, Sinha AK, Deering C and Briggs C (2010) A model for the origin of rhyolites from South Mountain, Pennsylvania: implications for rhyolites associated with large igneous provinces. *Lithosphere* **2**, 211–20.

Ross CS and Smith RL (1955) Water and other volatiles in volcanic glasses. *American Mineralogist* **40**, 1071–89.

Ross CS and Smith RL (1961) Ash-flow tuffs: their origin, geologic relations and identification. *US Geological Survey Professional Paper* **366**, 81 p.

Sahoo S, Chalapathi Rao NVC, Monie P, Belyatsky B, Dhote P and Lehmann B (2020) Petro-geochemistry, Sr-Nd isotopes and 40Ar/39Ar ages of fractionated alkaline lamprophyres from the Mount Girnar igneous complex (NW India): insights into the timing of magmatism and the lithospheric mantle beneath the Deccan large igneous province. *Lithos* **374–375**, art. 105712. doi: 10.1016/j.lithos.2020.105712.

Sahu NK and Karim MA (1993) On the occurrence of alkali basalts (basanitic) and alkaline felsic rocks around Kanesra, Rajkot district, Gujarat. *Indian Minerals* **47**, 219–28.

Schmincke H-U and Swanson DA (1967) Laminar viscous flowage structures in ash-flow tuffs from Gran Canaria, Canary Islands. *Journal of Geology* **75**, 641–64.

Self S (2006) The effects and consequences of very large explosive volcanic eruptions. *Philosophical Transactions of the Royal Society of London* **364**, 2073–97.

Sethna SF and Javeri P (2000) Essexite occurrence in the Deccan volcanic province of Saurashtra, western India. *Journal of Asian Earth Sciences* **18**, 151–4.

Sethna SF, Kothare P, Sethna BS and Javeri P (2001) Geology and petrography of the intrusives in the Deccan Trap of central and south-eastern Saurashtra, India. *Journal of Geological Society of India* **57**, 249–56.

Sheikh JM, Cucciniello C, Naik A, Sheth H and Duraiswami R (2023) Basaltic thermal and material inputs in rhyolite petrogenesis: the Chhapariyali rhyolite dyke, Saurashtra, Deccan Traps. *Geochemistry (Chemie der Erde)* **83**, art. 125984. doi: 10.1016/j.chemer.2023.125984.

Sheikh JM, Sheth H, Naik A and Keluskar T (2020a) Widespread rheomorphic and lava-like silicic ignimbrites overlying flood basalts in the northwestern and northern Deccan Traps. *Bulletin of Volcanology* **82**, art. 41. doi: 10.1007/s00445-020-01381-9.

Sheikh JM, Sheth H, Naik A and Keluskar T (2020b) Physical volcanology of the Pavagadh rhyolites, northern Deccan Traps: stratigraphic, structural, and textural record of explosive and effusive eruptions. *Journal of Volcanology and Geothermal Research* **404**, art. 107024. doi: 10.1016/j.jvolgeores.2020.107024.

Sheth H, Naik A, Sheikh JM and Kumar A (2022a) Giant (30 km-diameter) silicic caldera of K/Pg boundary age in the northwestern Deccan Traps: the Alech Hills, Saurashtra. *International Journal of Earth Sciences* **111**, 379–99.

Sheth H, Duraiswami RA, Ghule V, Naik A and Das T (2022b) Flood basalt structures and textures as guides to cooling histories and palaeoclimates: the Deccan Traps of Saurashtra, western India. *Geological Magazine* **159**, 1415–36.

Sheth HC, Choudhary AK, Bhattacharyya S, Cucciniello C, Laishram R and Gurav T (2011) The Chogat-Chamardi subvolcanic complex, Saurashtra, northwestern Deccan Traps: geology, petrochemistry, and petrogenetic evolution. *Journal of Asian Earth Sciences* **41**, 307–24.

Sheth HC, Zellmer GF, Kshirsagar PV and Cucciniello C (2013) Geochemistry of the Palitana flood basalt sequence and the eastern Saurashtra dykes, Deccan Traps: clues to petrogenesis, dyke-flow

relationships, and regional lava stratigraphy. Bulletin of Volcanology 75, art. 701. doi: 10.1007/s00445-013-0701-x.

Smith DB (1998) *Data compilation for USGS Reference Material QLO-1, Quartz Latite Oregon*. Washington, DC: US Geological Survey Open File Report.

Smith JV (2002) Structural analysis of flow-related textures in lavas. *Earth-Science Reviews* **57**, 279–97.

Smith JV and Houston EC (1994) Folds produced by gravity spreading of a banded rhyolite lava flow. *Journal of Volcanology and Geothermal Research* **63**, 89–94.

Snyder D (2000) Thermal effects of the intrusion of basaltic magma into a more silicic magma chamber and implications for eruption triggering. *Earth and Planetary Science Letters* **175**, 257–73.

Subba Rao S (1971) Petrogenesis of acid rocks of the Deccan Traps. *Bulletin of Volcanology* **35**, 983–97.

Szymanowski D, Ellis BS, Bachmann O, Guillong M and Phillips WM (2015) Bridging basalts and rhyolites in the Yellowstone-Snake River Plain volcanic province: the elusive intermediate step. *Earth and Planetary Science Letters* **415**, 80–9.

Tyrrell GW (1926) *The Principles of Petrology*. London: Methuen, 349 pp.

Vernon RH (2018) *A Practical Guide to Rock Microstructure*. 2nd edn. Cambridge: Cambridge University Press, 431 pp.

Wakhaloo SN (1967) On the nature of volcanic eruption and of differentiation of the Girnar igneous complex, Junagarh, Kathiawar peninsula, India. In *Proceedings of Symposium on the Upper Mantle Project*, National Geophysical Research Institute, Hyderabad, pp. 430–49.

Wolff JA and Wright JV (1981) Rheomorphism of welded tuffs. *Journal of Volcanology and Geothermal Research* **10**, 13–34.

Yatheesh V (2020) Structure and tectonics of the continental margins of India and the adjacent deep ocean basins: current status of knowledge and some unresolved problems. *Episodes* **43**, 586–608.

Yoder Jr HS (1973) Contemporaneous basaltic and rhyolitic magmas. *American Mineralogist* **58**, 153–71.

Zellmer GF (2021) Gaining acuity on crystal terminology in volcanic rocks. *Bulletin of Volcanology* **83**, art. 78. doi: 10.1007/s00445-021-01505-9.